Journal of Geotechnical and Geoenvironmental Engineering. Submitted September 5, 2012; accepted June 21, 2013; posted ahead of print June 24, 2013. doi:10.1061/(ASCE)GT.1943-5606.0000986

Dynamic Behaviour of Granulated Coal Ash during Earthquakes

Norimasa Yoshimoto[1)], Rolando P Orense, M. ASCE[2)], Masayuki Hyodo[3)] and Yukio Nakata[4)]

[1)] Assistant Professor, Dept. of Civil Engineering, Yamaguchi Univ., Tokiwadai 2-16-1, Ube, Yamaguchi, Japan. E-mail: nyoshi@yamaguchi-u.ac.jp

[2)] Associate Professor, Dept. of Civil Engineering, Univ. of Auckland, Private Bag 92019, Auckland 1142, New Zealand (corresponding author). E-mail: r.orense@auckland.ac.nz

[3)] Professor, Dept. of Civil Engineering, Yamaguchi Univ., Tokiwadai 2-16-1, Ube, Yamaguchi, Japan. E-mail: hyodo@yamaguchi-u.ac.jp

[4)] Professor, Dept. of Civil Engineering, Yamaguchi Univ., Tokiwadai 2-16-1, Ube, Yamaguchi, Japan. E-mail: nakata@yamaguchi-u.ac.jp

Journal of Geotechnical and Geoenvironmental Engineering. Submitted September 5, 2012; accepted June 21, 2013; posted ahead of print June 24, 2013. doi:10.1061/(ASCE)GT.1943-5606.0000986

Abstract:

Coal ashes discharged from coal-fired power plants have recently been gaining attention as a new form of geomaterials. They have been popularly used as ground materials for the improvement of unsuitable soil and for foam-mixed solidified soil. However, development of more applications is needed in the light of the enormous amount of coal ash generated. The present study was performed to confirm the applicability of granulated coal ash (GCA) as reclamation material with adequate resistance against liquefaction during an earthquake. In this study, the liquefaction characteristics of granulated coal ash was investigated through cyclic triaxial tests and online pseudo-dynamic response tests and the results were compared with those of natural sands to examine the cyclic shear properties of the material. The triaxial test results revealed that the slope of the cyclic shear strength curve of GCA was gentle under high confining pressure, but it was still higher than those of natural sands. It was observed that GCA underwent remarkable particle crushing, resulting in higher cumulative dissipated energy, and this accounted for the higher cyclic shear strength when compared to natural sand. Moreover, the online pseudo-dynamic response tests performed using a hollow torsional shear test apparatus showed that GCA exhibited slower excess pore water pressure build-up when compared to Toyoura sand for the same level of input motion. The presence of GCA layer in a saturated sandy ground had beneficial effects on the earthquake response.

Keywords:

granulated coal ash; earthquake; liquefaction; saturated sand; online pseudo-dynamic response test

Journal of Geotechnical and Geoenvironmental Engineering. Submitted September 5, 2012; accepted June 21, 2013; posted ahead of print June 24, 2013. doi:10.1061/(ASCE)GT.1943-5606.0000986

1. INTRODUCTION

In Japan, primary energy supply has increased steadily from about 16×10^{15} kJ in 1973 to about 24×10^{15} kJ in 2007. From these data, coal's contribution was about 15% in 1973 and 21% in 2007 (ANRE 2011). With such continuous rise in annual coal consumption due to increase in the energy demand, the amount of coal ash generated every year inevitably increases. In 2009, thermal power plants generate about 11 million tons of coal ash annually, up from the 8 million tons recorded ten years ago (JCOAL 2010). Therefore, it is necessary to look for options whereby coal ash can be utilized effectively. About 80% of the total amount of coal ash produced is being recycled, with the majority being used in cement production and in civil engineering works. Considering the latter, the utilization of coal ash is expected to increase from now on since large volume of ash could be used for engineering works at any given time.

The use of coal ash in civil engineering works, such as reclamation or backfill material, subgrade material, and soil improvement material, has already been reported by many researchers. For example, the applications of coal ash to geotechnical engineering have been investigated by Horiuchi et al. (1992; 1995) and Sawa et al. (2002).

The authors have been studying the mechanical properties of granulated coal ash (GCA) formed by milling process, with small amount of cement added and whose particle size is almost equivalent to that of sand or fine gravel (Yoshimoto et al., 2005, 2006, 2007, 2008). Granulation results in improved work efficiency, and because dispersion is prevented, the material is convenient to store. The material can be handled in the same manner as ordinary soil. The use of GCA has many advantages, such as the suppression of leaching of heavy metals and the possibility of outdoor curing.

Journal of Geotechnical and Geoenvironmental Engineering. Submitted September 5, 2012; accepted June 21, 2013; posted ahead of print June 24, 2013. doi:10.1061/(ASCE)GT.1943-5606.0000986

This research was performed to confirm the applicability of GCA as reclamation material with adequate resistance against liquefaction during earthquake. Because of its different index properties, it is believed that the seismic response characteristics of granulated coal ash during earthquakes are different from those of natural sand. Therefore, a series of cyclic triaxial tests was carried out on specimens of GCA to evaluate the cyclic shear strength of this material. Moreover, online pseudo-dynamic response tests were performed to understand the dynamic response characteristics of GCA. The results were than compared to those of Toyoura sand.

2. MATERIALS USED

Granulated coal ash is a material that is modified by adding cement, water and additives to the coal ash, and the mixture is granulated by mixing and rotating. The granulated coal ash used in the test, consisting of 85% coal ash, 5% cement and 10% additives by weight, was manufactured using a motor mixer with 10 m^3 capacity. The material was cured under water content of w=40%. Because of the limitation of the testing device, the particle size used was less than 2.0 mm. The appearance of granulated coal ash is shown in Figure 1. It can be observed that granulated coal ash looks similar to ordinary sand or fine gravel, with round-shaped particles.

Table 1 shows the physical properties of GCA used in this study. In the table, ρ_s is the particle density, e_{max} and e_{min} are the maximum and minimum void ratios, respectively, and d_{50} is the mean particle diameter. The parameters R_c, and A_r are the roundness coefficient and aspect ratio, respectively, and they are indices that describe the particle shape. In this study, $R_c=L^2/4\pi A$ where L is the perimeter measured on plan images of particles arranged in their most stable position and A is the cross-sectional area of the same image. This coefficient is equal to unity for a perfectly circular particle and becomes >1 with increasing particle roughness. On the other hand, $A_r=b/a$ where a and b are widths of the particle along the minor and major axes, respectively. For comparison purposes,

Journal of Geotechnical and Geoenvironmental Engineering. Submitted September 5, 2012; accepted June 21, 2013; posted ahead of print June 24, 2013. doi:10.1061/(ASCE)GT.1943-5606.0000986

the properties of five types of natural soils which were used in this study are also shown in the table. Toyoura is a standard silica sand commonly used in laboratory testing in Japan. Port Island (P.I.) Masado is weathered decomposed granite soil used in the reclamation of artificial islands in Kobe, and which was extensively investigated following the 1995 Kobe earthquake. Aio and Wakasa are beach sands found in Yamaguchi Prefecture (in southwest part of Japan) and Fukui Prefecture (in central Japan), respectively. Iwakuni clay was taken from Iwakuni City in Yamaguchi Prefecture. These natural soils were considered because they were extensively investigated in the Geotechnical Engineering Laboratory, Yamaguchi University. A special soil, Shirasu with fines content F_c=10%, was included which has similar grain size distribution as the GCA. This will be referred to in this paper simply as "Shirasu".

The specific gravity of the particles of GCA is very low because of the presence of air vesicles in individual grains. In particular, the maximum and minimum void ratios of GCA, which were determined using the methods specified in the Japanese Geotechnical Society standard (JGS, 2000), were found to be very large as compared to natural soils. The particle size distribution curves depicted in Figure 2 show practically similar curves for GCA, Shirasu and Port Island (P.I.) Masado. These materials contain about 10~20% fines and are well-graded with high coefficient of uniformity.

3. UNDRAINED CYCLIC TRIAXIAL TESTS

In this section, the results of a series of undrained cyclic triaxial tests conducted on granulated coal ash is presented, together with the comparison of its undrained cyclic shear behavior with those of natural sands.

3.1 Specimen Preparation

Journal of Geotechnical and Geoenvironmental Engineering. Submitted September 5, 2012; accepted June 21, 2013; posted ahead of print June 24, 2013. doi:10.1061/(ASCE)GT.1943-5606.0000986

The particles of granulated coal ash have large surface voids. In order to saturate the materials, samples were placed in de-aeration tank for 2-3 days to remove the air bubbles. Then, to prepare the test specimens, GCA was water-pluviated into a mould which was then gently tapped until the required relative density was achieved. The specimens were then saturated until a B-value > 0.96 was achieved. Specimens were isotropically consolidated to 50, 100, 200, 300, and 400 kPa. For natural sands, samples were air-pluviated into a mould which was then gently tapped to obtain the target relative density, followed by saturation with appropriate back pressure and then isotropically consolidated to 100 kPa. For these materials, a sinusoidal cyclic axial load was applied in the test at a frequency of 0.1Hz under undrained condition. In contrast, cyclic triaxial tests on Iwakuni clay were carried out at confining pressure of 100kPa with a frequency of 0.02 Hz. Since it takes time for the pore water pressure to propagate within the clay specimen, a slower loading frequency was adopted for clays to ensure uniform distribution of pore water pressure. Hyodo et al (1994) investigated the dependency of cyclic shear strength on the frequency of loading on clay samples and the results indicate that the effect of loading frequency disappeared when the frequency is less than 0.02Hz.

3.2 Cyclic Shear Behaviour

Figure 3 shows the plots of double amplitude axial strain ε_{DA} and residual pore pressure ratio u_r/σ_c' against normalized number of cycles N/N(at ε_{DA}=5%) obtained from undrained cyclic shear tests on GCA specimens (relative density, D_r=50%) corresponding to σ_c' = 50, 100, 200, 300 and 400kPa. Because of the different cyclic shear stress ratios involved, it was deemed best to present the comparison through this plot. Note that the Martin and Seed (1978) identified excess pore water pressure generation in the same way. The curves for each residual pore pressure ratio, u_r/σ_c', show practically similar behaviour, while those corresponding to double amplitude axial strain ε_{DA} are

Journal of Geotechnical and Geoenvironmental Engineering. Submitted September 5, 2012; accepted June 21, 2013; posted ahead of print June 24, 2013. doi:10.1061/(ASCE)GT.1943-5606.0000986

dispersed, with the variation dependent on the level of confining pressure. In the case of high confining pressure, there is significant development of ε_{DA} even from the start of cyclic loading.

The cyclic shear behaviour of granulated coal ash at relative density, D_r=50% is then compared with natural soils of the same density on the basis of double amplitude axial strain ε_{DA}, residual pore pressure ratio u_r/σ_c' and cumulative dissipated energy ΣW.

The relationship between normalized number of cycles N/N(at ε_{DA}=5%) and double amplitude axial strain ε_{DA} is presented in Figure 4. Again, this is a better way to compare the results because, as mentioned earlier, these materials were tested under different loading frequencies and only through this way could a meaningful comparison be done. Note that because cyclic shear strengths greatly differ for each material, the results for ε_{DA}=5% corresponding to 20 cycles are shown next to the sample name indicated in the explanatory notes in Figure 4. In the case of natural sands, axial strain did not occur at the early stage of cyclic loading; however, at strain level of about ε_{DA}=5%, it suddenly increased to almost the maximum values at N/N(at ε_{DA}=5%) of about 0.9 to 0.95. Conversely, axial strain in Iwakuni clay increased almost constantly from the start of cyclic loading. It can be seen that the result corresponding to GCA shows intermediate behaviour between these two types of soil.

The cumulative dissipated energy ΣW is indicated by the area under the cyclic stress-strain curve obtained from the relation between deviator stress and axial strain, as shown in Figure 5. Towhata and Ishihara (1985) used this concept to evaluate cyclic shear behaviour and liquefaction strength. Note that the cumulative dissipated energy ΣW is the energy consumed by the soil during plastic deformation until liquefaction. Thus, the energy absorption capacity is high when this value is large, and consequently, the liquefaction strength would also be high. Figure 6 shows the plot of cumulative dissipated energy ΣW against double amplitude axial strain ε_{DA} for all the materials

Journal of Geotechnical and Geoenvironmental Engineering. Submitted September 5, 2012; accepted June 21, 2013; posted ahead of print June 24, 2013. doi:10.1061/(ASCE)GT.1943-5606.0000986

tested. Based on the figure, ΣW of GCA is about two or three times higher than those of natural sands, while it is about 50 percent lower than that of Iwakuni clay.

Figure 7 shows the relation between normalized number of cycles N/N(at ε_{DA}=5%) and residual pore pressure ratio u_r/σ_c' for all the materials tested. Natural sands and Iwakuni clay initially show almost similar behaviour of constantly increasing pore pressure ratio with the number of cycles from the start of cyclic loading. For sands, however, the pore pressures are triggered to increase suddenly at about N/N(at ε_{DA}=5%) = 0.8, and continue to increase until a value equal to the initial effective confining stress is reached. This is typical of liquefaction behaviour. In the case of GCA, the pore pressure development is large from the start of cyclic loading. However, the pore pressure does not increase up to the initial effective confining stress.

The same data is presented in Figure 8 in terms of the relation between cumulative dissipated energy ΣW and residual pore pressure ratio u_r/σ_c'. Sands are not resistant to liquefaction because they lack energy absorption capacity. In contrast, the residual pore pressure ratio in Iwakuni clay increased only up to about u_r/σ_c'=0.6, corresponding to a double amplitude axial strain ε_{DA} = 5%. It is also observed that natural sands and GCA show similar behaviour until u_r/σ_c' = 0.6; however, in the case of GCA, u_r/σ_c' does not reach 1.0 when ε_{DA} = 5%. Granulated coal ash is therefore more resistant to liquefaction than natural sands.

3.3 Cyclic Shear Resistance

Figure 9(a) shows the cyclic resistance curves of GCA (D_r=5%) at double amplitude axial strain ε_{DA}=5% for various confining pressures. The curve is steep when the confining pressure is 50 kPa. As the confining pressure increases to 400kPa, the corresponding curve becomes flatter. This observation is consistent with those observed in natural sands where the liquefaction resistance decreases as the confining pressure is increased, as pointed out by many researchers (e.g. Rollins

Journal of Geotechnical and Geoenvironmental Engineering. Submitted September 5, 2012; accepted June 21, 2013; posted ahead of print June 24, 2013. doi:10.1061/(ASCE)GT.1943-5606.0000986

and Seed, 1988; Boulanger and Idriss, 2004). Thus, granulated coal ash appears to follow the same trend although the effect is less pronounced. As will be discussed later, GCA is more crushable than natural geomaterials and therefore there is a need to look more closely on the effect of confining pressure on the liquefaction resistance breakage of GCA.

The comparison of cyclic shear resistance of granulated coal ash with those of natural soils at the same density (D_r=50%) is presented in Fig. 9(b). The cyclic deviator stress ratio of granulated coal ash is about 1.5~2.5 times higher than those of natural sands and almost similar to that of Iwakuni clay. Note that in general, the cyclic deviator stress ratio to cause failure after 15~20 cycles is defined as liquefaction resistance. Thus, the liquefaction resistance of GCA is about 1.7 times higher than that of Toyoura sand.

In order to discuss the cyclic shear strength of GCA, we paid attention to particle breakage during the test. Another series of tests was terminated at different stages and sieve analyses were carried out: (1) on the original samples; (2) after the end of consolidation but before cyclic shear; and (3) after the end of cyclic shear. A typical set of results is shown in Figure 10 for the original (virgin) sample and for two other samples consolidated at σ_c'=100kPa. It can be seen that the particle size distributions of the two samples are different when compared to that of original sample, with obvious increase in size of smaller particles. The same data is presented in Figure 11(a) in the form of a bar chart showing the percentage increase for each sieve size at each stage of testing. An increase in the percentage of smaller-sized particles represents breakage of larger-sized particles. Examination of the figure indicates that particle breakage is more significant after the shearing stage than after consolidation stage (i.e. before shearing) and such increase is more evident for smaller-sized particles. When both are added, the total percentage increase due to particle breakage during the test is known. This reaches a maximum value of 9%.

Journal of Geotechnical and Geoenvironmental Engineering. Submitted September 5, 2012; accepted June 21, 2013; posted ahead of print June 24, 2013. doi:10.1061/(ASCE)GT.1943-5606.0000986

An attempt was made to quantify the degree of particle crushing in terms of the increase in the surface area of the particles at different stages of the tests. For this purpose, the method proposed by Miura and Yamanouchi (1971) was used which involves the estimation of the surface area of the particles within the triaxial specimen. The specific surface of the particles was measured by first sieving the soil using different sieve sizes. For the range of particle sizes investigated, the specific surface area, S, (in cm^2/cm^3) is calculated as:

$$S = \sum \frac{F}{100} \cdot \frac{4\pi \left(d_m/2\right)^2}{(4/3)\pi \left(d_m/2\right)^3 G_s \gamma_w} \cdot \gamma_d \qquad (1)$$

where $d_m = \sqrt{(d_1 \cdot d_2)}$, d_1 and d_2 are adjacent sieve sizes, F is the % by weight retained on the sieve, G_s is the specific gravity of the particles, γ_w is the unit weight of water and γ_d is the dry unit weight of the specimen. The change in specific surface area, ΔS (in cm^2/cm^3), before and after cyclic shear is calculated as

$$\Delta S = S_{after} - S_{before} \qquad (2)$$

Figure 11(b) compares the increase in specific surface area within the specimens before and after shearing at different effective confining pressures. It is seen from the figure that at any confining pressure, the degree of particle crushing after cyclic shear, as manifested by the increase in surface area, is more significant than that after isotropic consolidation; this trend generally increases with higher confining pressure. Thus, it can be said that particle breakage is caused more by the application of shear stresses, rather than by normal stress.

3.4 Discussion

Journal of Geotechnical and Geoenvironmental Engineering. Submitted September 5, 2012; accepted June 21, 2013; posted ahead of print June 24, 2013. doi:10.1061/(ASCE)GT.1943-5606.0000986

In general, it is known that grain size distribution, density and particle shape of material significantly affects the cyclic shear resistance. Yamawaki et al. (2002) carried out cyclic undrained triaxial tests for two kinds of materials with similar grain size distribution and relative density. They reported that as the roundness coefficient or aspect ratio (the asperity of particle shape) increases, the cyclic shear strength also increases. Along this line, a series of tests was conducted in this study on Shirasu and granulated coal ash with similar grain size distribution and relative density. Because the roundness coefficient or aspect ratio of Shirasu is larger than that of granulated coal ash (see Table 1), it is expected that cyclic shear strength of Shirasu would be higher than that of granulated coal ash. However, as shown in Figure 9(b), the cyclic deviator stress ratio of granulated coal ash is about 1.5 or 2.0 times higher than that of Shirasu. Under the confining pressure considered, GCA undergoes remarkable particle crushing, as indicated in Figures 10 and 11. In the case of Shirasu, on the other hand, the increase in percent finer by weight is only about 2% (Hyodo, 2002). Thus, particle crushing in Shirasu does not occur easily as compared to granulated coal ash. For GCA, cyclic shearing results in particle crushing, and the soil structure is gradually stabilized. This results in the cyclic shear resistance of GCA exceeding that of Shirasu. In similar vein, the cyclic strength of GCA is larger than that of natural sand because some energy is spent during the particle crushing of GCA as illustrated in Figures 6 and 8, leading to its higher cumulative dissipated energy.

It has been mentioned that both confining pressure and particle crushing play significant role in the liquefaction resistance of GCA. From the discussion presented earlier, particle breakage is caused more by the application of shear stress, rather than by normal stress. Particle breakage results in a more stable soil skeleton, thereby increasing the liquefaction resistance. Thus, although there is confining pressure dependency of the liquefaction resistance of granulated coal ash, such effect is weakened by the particle crushing induced during cyclic shearing.

It has been a common perception in geotechnical engineering that contractive behaviour will lead to pore pressure increase. Since crushable particles are contractive, then they should be more

Journal of Geotechnical and Geoenvironmental Engineering. Submitted September 5, 2012; accepted June 21, 2013; posted ahead of print June 24, 2013. doi:10.1061/(ASCE)GT.1943-5606.0000986

liquefaction-prone. However, as the results indicated, crushable materials have higher liquefaction resistance. This is because, as discussed earlier, when particles break during cyclic shear, the points of contact between particles increase and with continuous load application, a more stable soil skeleton is formed, thereby increasing the shear resistance when compared to natural sands. Similar results were obtained in other materials which are crushable, such as Toyoura sand under very high confining pressure (Hyodo et al., 2000) and pumice sand (Orense et al. 2012).

Looking back at Figure 7, it can be seen that for GCA specimen, there is significant increase in pore water pressure during the 1st cyclic load application, indicating that indeed, particle crushing leads to a contractive response. However, once the particle is crushed, subsequent cyclic load application results in more particle crushing leading to the formation of more stable soil skeleton. In addition, the increase in contact surfaces caused by crushing provides interlocking effect on the particles. This results in a more controlled development of pore water pressure, i.e., the rate of change of pore water pressure decreases with number of cycles, as indicated in the figure. This is opposite to that observed in other natural sands where the rate of increase is gradual in the early stage of cyclic load application, followed by an increase in the rate at the latter stage.

Additional tests were performed on GCA specimens under different initial relative densities and also under different over-consolidation ratios (OCR). The results of these tests are not presented here for brevity, but they are included in the electronic supplement. The results confirmed similar effect of particle crushing on the liquefaction resistance of GCA specimens.

4. ONLINE PSEDO-DYNAMIC TESTS

Journal of Geotechnical and Geoenvironmental Engineering. Submitted September 5, 2012; accepted June 21, 2013; posted ahead of print June 24, 2013. doi:10.1061/(ASCE)GT.1943-5606.0000986

Next, online pseudo-dynamic response tests were performed on granulated coal ash using a hollow torsional shear test apparatus. For comparison purposes, similar tests were performed using Toyoura sand, and the difference in the seismic response of the two materials is presented below.

4.1 Basic Concept

Online testing is a method of modeling earthquake effects by obtaining soil response characteristics directly from soil samples rather than by multi-parameter constitutive models. It involves conducting both laboratory element tests and seismic response analysis in series within each time step. The principle of the online pseudo-dynamic response test for the analysis of level ground is shown in Figure 12. The system, which was initially developed by Kusakabe et al. (1990), involves the following algorithm. First, the ground to be analyzed is converted into a series of lumped mass models subjected to an earthquake excitation at the base (Figure 12a). Next, the dynamic excitation of the mass system is solved using a computer to determine the displacement response of each mass. The shear strain that is equivalent to the resultant displacement is applied to the corresponding specimen under computer control. The restoring forces that are monitored for each soil specimen are then used to calculate the displacement response for the next step (Figure 12b). This process is then repeated for as long as the earthquake motion continues in order to directly determine the constantly changing non-linear restoring force of the ground from the element tests.

Online testing as a one-dimensional method has limitations in its application to practical problems. However, the accuracy of the analysis is not problematic compared with conventional numerical procedures (Takahashi et al., 2006). The online testing method has several advantages in analyzing the one-dimensional seismic response of grounds when compared for example to 1g dynamic model testing. Aside from taking into account the scale effects on liquefaction and the easy application of actual earthquake records, online testing combines the best features of both laboratory element

Journal of Geotechnical and Geoenvironmental Engineering. Submitted September 5, 2012; accepted June 21, 2013; posted ahead of print June 24, 2013. doi:10.1061/(ASCE)GT.1943-5606.0000986

testing and numerical algorithms to determine the soil response characteristics directly from soil samples.

In the tests presented herein, the element experiment was conducted using a hollow torsional shear test apparatus. In performing the dynamic analysis, the following equations were solved:

$$M\ddot{x} + C\dot{x} + F = -MLA_{ccg} \quad (1)$$

where M is the mass matrix; C is the damping matrix, F is the restoring force vector; L is a unit vector; A_{ccg} is the input acceleration vector and x is the displacement vector. Some form of viscous damping is used in the nonlinear analysis to provide for damping at very small strains where the hysteretic damping from the non-linear soil models is nearly zero (Murono and Tanamura, 2001; Kwok et al., 2006). The damping is modeled using Rayleigh damping parameters with damping coefficients proportional to the mass and stiffness. The Rayleigh parameters were computed to give the required levels of viscous damping at two different frequencies, herein the first and second modes of free vibration, with target damping ratio set at 5% (Park and Hashash, 2004). The linear acceleration method was used for the initial numerical integration and the central difference method was then used in subsequent steps (Shibata, 1981).

4.2 Model Ground

For the online pseudo-dynamic response tests, the soil profile at the location of the seismometer array in Port Island, which liquefied extensively during the 1995 Hyogoken Nanbu Earthquake, was employed (Kobe City Development Authority, 1995). The horizontally layered ground, with total depth of 33 m, was divided into 4 layers, each of which was replaced by a one-dimensional mass model (m_1 to m_4). Instead of the original decomposed granite soil (Masado), the 16 m-thick

Journal of Geotechnical and Geoenvironmental Engineering. Submitted September 5, 2012; accepted June 21, 2013; posted ahead of print June 24, 2013. doi:10.1061/(ASCE)GT.1943-5606.0000986

liquefiable layer was replaced by either granulated coal ash layer or by Toyoura sand layer, as shown in Figure 13. Note that the properties of Masado have been extensively investigated by many researchers (Hyodo et al., 1997; Fukushima et al., 2001). In the tests, only the ground elements that were likely to be prone to liquefaction and excessive deformation were tested to determine the restoring force; these were referred to as "online layer". The restoring forces of the other layers were estimated numerically by introducing "analytical layers". The response of the whole system is analyzed as in any one-dimensional seismic response analysis; hence, equilibrium among all the layers is guaranteed. Due to the limitation of the number of testing equipment, only one layer (S_2) was considered as online layer (where restoring forces are determined), while the rest of the layers are treated as analytical layer (using modified R-O model).

The analytical parameters chosen for the modified Ramberg-Osgood models are also shown in Figure 13. These values were taken as similar to those of the original ground, as reported in the literature (e.g., Yamaguchi et al. 2002). Since the S_2 layer was replaced by either Toyoura sand or granulated coal ash, the parameters of the underlying layers (S_3 and S_4) have to be modified to account for the changes in confining pressure due to the different unit weights of granulated coal ash and Toyoura sand. For example, the initial shear moduli were assumed to be proportional to $(\sigma_c')^{0.5}$, where σ_c' is the effective confining pressure (Iai et al., 1990).

4.3 Element Experiments

The element test was carried out using a hollow torsional shear apparatus. Shearing was carried out under undrained conditions assuming zero vertical and volumetric strains. The load was applied using mega-torque motor with maximum capacity of 260 N-m and maximum rotating speed of 28 rpm. For the tests presented herein, the shear strain rate was set at 0.1%/min. Although this is quite less than real time rates, it is commonly accepted that liquefaction and cyclic mobility of sands are

Journal of Geotechnical and Geoenvironmental Engineering. Submitted September 5, 2012; accepted June 21, 2013; posted ahead of print June 24, 2013. doi:10.1061/(ASCE)GT.1943-5606.0000986

dependent on the number of cycles and level of normalized shear stress and independent of frequency (Ishihara, 1993).

The GCA specimens in the element tests were prepared using water pluviation technique, while the Toyoura sand specimens were formed using air pluviation method, followed by saturation with appropriate back pressure. For both specimens, full saturation was confirmed by checking the B-value. The model specimens, measuring 70 mm high with 35 mm and 70 mm inner and outer diameters, respectively, have initial relative densities of D_r=60%. They were consolidated isotropically to an effective confining pressure equal to the overburden stress at the midpoint of S_2 layer (see Figure 13).

4.4 Input motion

For the reference earthquake input motion, the acceleration record observed at location PI-33m NS (maximum acceleration of α_{max}=544 cm/s^2) at a depth of 33 m of the seismic array in Kobe Port Island during the 1995 Hyogoken Nambu Earthquake was used (see Figure 14). In the online tests, four (4) levels of input motions were considered, i.e., with maximum amplitudes of 30%, 50%, 70% and 100% of the reference earthquake motion, in order to investigate the seismic response of the model grounds to various degrees of excitations.

4.5 Test Results and Discussion

Typical results of the online pseudo-dynamic response tests are shown in Figure 15, where the acceleration time histories at the surface of each layer (S_1 - S_4) for model grounds containing GCA and Toyoura sand are illustrated corresponding to an input acceleration equal to 100% of the reference input motion. It can be observed that the acceleration response for S_3 and S_4 layers are almost similar, and characterized by high frequency components. However, as the earthquake wave

Journal of Geotechnical and Geoenvironmental Engineering. Submitted September 5, 2012; accepted June 21, 2013; posted ahead of print June 24, 2013. doi:10.1061/(ASCE)GT.1943-5606.0000986

propagated through S_2 layer, the acceleration underwent different degrees of de-amplification accompanied by filtering of the high frequency components. These phenomena are associated with the liquefaction of S_2 layer. The accelerations on the ground surface were almost similar for both model grounds.

To verify that indeed S_2 layer had liquefied, the shear stress-shear strain relations are plotted for both granulated coal ash and Toyoura sand layers, and these are shown in Figure 16. It can be seen that Toyoura sand underwent stiffness degradation followed by the development of large deformation after only a few number of cyclic load application. Similar pattern was observed for granulated coal ash, although large deformation occurred after a greater number of cycles. These large deformations and reduction in stiffness of the grounds are indications of the occurrence of soil liquefaction.

Succeeding online test results for other amplitudes of input acceleration showed that Toyoura sand layer would liquefy if the acceleration amplitude exceeds 50% of the reference earthquake motion. On the other hand, test results for granulated coal ash indicated that it will liquefy only if the amplitude is equal to 100% of the reference earthquake motion. For comparison purposes, Figure 17 shows the shear stress-shear strain relations for both materials at an input acceleration equal to 70% of reference motion. Note that these represent the actual response of the soils, as obtained from cyclic torsional shear tests. It can be observed that while Toyoura sand showed stiffness degradation after a few cycles followed by development of large strain, the stress-strain relation for granulated coal ash showed otherwise, with much stiffer response as the cyclic loading progressed, and therefore, smaller deformation.

Next, the development of excess pore water pressure in both layers is examined for the case of input motion with 70% and 100% of the reference acceleration, and the time histories are shown in Figure 18. For both amplitudes of acceleration, Toyoura sand reached very high excess pore water pressure,

Journal of Geotechnical and Geoenvironmental Engineering. Submitted September 5, 2012; accepted June 21, 2013; posted ahead of print June 24, 2013. doi:10.1061/(ASCE)GT.1943-5606.0000986

although the generation of pore pressure was faster for the higher level of acceleration. For granulated coal ash, on the other hand, very high pore water pressures were obtained when the acceleration was 100% of the reference value, but a lower degree of pore pressure build-up can be seen when the amplitude was 70% of the reference value. The latter case indicated that liquefaction did not occur.

The acceleration response spectrum of the input motion corresponding to 5% damping is compared with those obtained at the ground surface for both model grounds subjected to acceleration amplitude of 70% of the reference motion, and these are shown in Figure 19(a). It can be seen that the predominant period of the input motion is around 0.7 sec. In the case of Toyoura sand, liquefaction occurred at this level of acceleration and, as a result, the predominant period shifted to about 1.5 sec, indicating softening of the S_2 layer. On the other hand, the predominant period for granulated coal ash moved to about 4 sec. Although granulated coal ash did not undergo complete liquefaction, as indicated in Figure 18(b), the material softened to such a degree that the period has shifted to a higher level. Note that in both cases, the high frequency components of the base motion have been filtered through the softened grounds.

A comparison of the vertical distributions of the response displacement (relative to the base displacement) of Toyoura sand and granulated coal ash is shown in Figure 19(b), corresponding to an input motion with amplitude equal to 70% of the reference acceleration. It can be seen that, as expected, larger shear strain and therefore larger displacement occurred in S_2 layer consisting of Toyoura sand due to the complete liquefaction of the said layer. On the contrary, since the granulated coal ash did not completely liquefy, the relative displacement at the top was smaller when compared to Toyoura sand.

The effectiveness of granulated coal ash is illustrated in Figure 20, which compares the maximum excess pore water pressure ratio and maximum displacement for different levels of input

Journal of Geotechnical and Geoenvironmental Engineering. Submitted September 5, 2012; accepted June 21, 2013; posted ahead of print June 24, 2013. doi:10.1061/(ASCE)GT.1943-5606.0000986

accelerations of GCA and Toyoura sand as layer S_2. Although both layers would liquefy when subjected to the full amplitude of the reference acceleration recorded during the Kobe earthquake, the granulated coal ash layer would not liquefy when the acceleration is reduced to less than 70% of the reference value. On the other hand, Toyoura sand will liquefy even if the input motion is only 50% of the reference amplitude, with large ground displacements generated.

Note that, as the results indicated, both GCA and Toyoura sand would liquefy when subjected to a very high excitation, such as the one experienced in Kobe when the reclaimed soil (consisting of PI Masado) liquefied. However, under lower level of excitation (say 70% of Kobe-class motion), GCA will not liquefy but Toyoura sand would. Based on the results presented, it is can be said that the granulated coal ash would perform better as reclamation material than Toyoura sand (or even P.I. Masado, whose liquefaction resistance is similar to Toyoura sand) when subjected to the specified earthquake excitation. This is consistent with the findings from cyclic triaxial tests that the liquefaction strength of GCA was about 1.7 times higher than that of Toyoura sand. These confirm the effectiveness of granulated coal ash as backfill/reclamation material for use in waterfront areas.

6. CONCLUSIONS

This research was performed to confirm the applicability of granular coal ash as reclamation material with adequate resistance against liquefaction during earthquake. For this purpose, cyclic undrained triaxial tests and online pseudo-dynamic response tests were performed to investigate the cyclic undrained behavior and seismic response characteristics of GCA in comparison with natural sands. Based on the results presented herein, the following are the major conclusions obtained.

(1) The pore pressure and deformation response of granulated coal ash showed intermediate behaviour between sand and clay. GCA underwent considerable particle crushing during cyclic triaxial testing.

Journal of Geotechnical and Geoenvironmental Engineering. Submitted September 5, 2012; accepted June 21, 2013; posted ahead of print June 24, 2013. doi:10.1061/(ASCE)GT.1943-5606.0000986

(2) The liquefaction resistance of GCA is about 1.7 times higher than that of Toyoura sand. The cyclic deviator stress ratio of granulated coal ash is almost the same as that of Iwakuni clay.

(3) The cumulative dissipated energy for GCA is larger than that of natural sand because some energy was spent as the particles undergo crushing. It is believed that this is the reason why the cyclic shear strength of granulated coal ash is higher than that of natural sand.

(4) From the online tests, the presence of granulated coal ash layer in the model ground resulted in shifting of the predominant period of the surface acceleration to a higher value, at least within the range of the amplitude of input acceleration investigated.

(5) The online tests confirmed that GCA showed slower excess pore water pressure build-up when compared to Toyoura sand for the same level of input motion.

(6) Although the excess pore water pressure increased as the amplitude of the input acceleration increased, the response displacement of model ground with GCA layer was smaller when compared to that with Toyoura sand layer.

Note that the paper focused on the results of the basic research on the cyclic properties of granulated coal ash. When implementing GCA in real practice, such as in reclamation work and backfilling projects, it is necessary to investigate the effects of other factors, such as static settlement, long-term performance and environmental impact among others. Thus, future research is recommended to clarify the effect of these factors.

Journal of Geotechnical and Geoenvironmental Engineering. Submitted September 5, 2012; accepted June 21, 2013; posted ahead of print June 24, 2013. doi:10.1061/(ASCE)GT.1943-5606.0000986

REFERENCES

Agency for Natural Resources and Energy, ANRE (2011). *Energy in Japan 2010*, http://www.enecho.meti.go.jp/index_backpamph.htm

Boulanger, R.W & Idriss, I.M. (2004). "State normalization of penetration resistances and the effect of overburden stress on liquefaction resistance." *Proc., 11th Int Conf on Soil Dynamics and Earthquake Engineering and 3rd Int Conf on Earthquake Geotechnical Engineering*, Vol. 2, 484-491.

Fukushima, S. and Mochizuki, Y. (2001). "Effects of density and confining stress on liquefaction resistance of coarse-grained reclaimed soils used for construction of man-made islands in Kobe," *Journal of Geotechnical Engineering, JSCE*, No.687, 49-64 (in Japanese).

Horiuchi, S., Taketsuka, M., Odawara, T. and Kawasaki, H. (1992). "Fly-Ash Slurry Island: I Theoretical & experimental investigations," *J. Materials in Civil Eng*. ASCE, 117-133 (in Japanese).

Horiuchi, S., Tamaoki, K. and Yasuhara, K. (1995). "Coal ash slurry for effective underwater disposal," *Soils and Foundations*, 35(1), 1-10.

Hyodo, M., Sugiyama, M., Yamamoto, Y. and Kawata, Y. (1994). "Evaluation of pore pressure and strain of normally consolidated and overconsolidated clay subjected to cyclic shear stress," *Journal of Geotechnical Engineering, JSCE*, No.487, 79-88 (in Japanese).

Hyodo, M., Aramaki, N., Tokuhara, Y., Kikuchi, S., Nakata, Y. and Murata, H. (1997). "Undrained cyclic shear characteristics of decomposed granite soil in Rokko Island," *Journal of Geotechnical Engineering, JSCE*, No.582, 87-98 (in Japanese).

Hyodo, M., Nakata, Y., Aramaki, N., Hyde, A.F.L. and Inoue, S. (2000). "Liquefaction and particle crushing of soil," *Proc. 12th World Conference on Earthquake Engineering*, Auckland, New Zealand, Paper 0278, 8pp.

Hyodo, M. (2002). "Effect of fines on compression, shear and particle breakage characteristics of volcanic soil 'Shirasu'," *Proceedings of the Symposium on Evaluation Method of Engineering Characteristics of Volcanic Grounds*, 129-140 (in Japanese).

Iai, S., Matsunaga, Y. and Kameoka, T. (1990). "Strain space plasticity model for cyclic mobility," *Report of the Port and Harbour Research Institute*, 29:4.

Ishihara, K. (1993). Liquefaction and flow failures during earthquakes. *Geotechnique* 43:3, 351-415.

Japan Coal Energy Center, JCOAL (2010). *Volume of Coal Ash Generation (FY 1997-2009)* http://www.jcoal.or.jp/coalash/ash01.html

Japanese Geotechnical Society (2000). *Soil Test Procedures and Commentaries*, First Revised Edition, Tokyo (in Japanese).

Kobe City Development Authority (1995). *Investigation of the deformation of reclaimed land (Port Island and Rokko Island) during the 1995 Hyogoken-Nambu Earthquake*, Report (in Japanese).

Kusakabe, S., Morio, S. and Arimoto, K. (1990). Liquefaction phenomenon of sand layers by using online computer test control method. *Soils and Foundations* 30:3, 174-184.

Kwok, O.A., Stewart, J.P., Hashash, Y,M.A., Matasovic, N., Pyke, R., Wang, Z.L. Yang, Z.H. (2006). "Practical implementation of analysis routines for nonlinear seismic ground response analysis," *Proc., 8th U.S. National Conference on Earthquake Engineering*, Paper No. 546, 10pp.

Martin, P.P. and Seed, H.B. (1978). "APOLLO: A computer program for the analysis of pressure generation and dissipation in horizontal sand layers during cyclic or earthquake loading," *Report No. UBC/EERC-78/21*, University of California, Berkeley.

Murono, Y. and Tanamura, S. (2001). "Effects of Rayleigh damping in non-linear response analysis of soil layer," *Railway Technical Research Institute Report*, Vol. 15, No. 3, 23-28 (in Japanese).

Orense, R.P., Pender, M.J. and Tai, A. (2012). "Undrained cyclic shear behaviour of pumice sand," *Proc., Australia-New Zealand Conference on Geomechanics*, 6pp.

Park, D. and Hashash, Y.M.A. (2004). "Soil damping formulation in nonlinear time domain site response analysis." *Journal of Earthquake Engineering*, Vol. 8, No. 2, 249-274.

Rollins, K.M. and Seed, H. B. (1988). "Influence of buildings on potential liquefaction damage." *Journal of Geotechnical Engineering, ASCE*, 116, GT2, 165-185.

Sawa, K., Tomohisa, S., Maruyama, S. and Ogawa, A. (2002). "Strength characteristics of cement-treated sludge mixed with coal fly ash," *Journal of the Society of Materials Science*, 51(1), 30-35 (in Japanese).

Shibata, A. (1981). *Recent Earthquake Resistant Structural Analyses*, Morikita Shuppan Co., Tokyo (in Japanese).

Takahashi, N. Hyodo, M., Hyde, A.F.L., Yamamoto. Y. and Kimura, S. (2006). On-line earthquake response test for stratified layers of clay and sand. *Journal of Geotechnical and Geoenvironmental Engineering*, ASCE 132:5, 611-621.

Towhata, I. and Ishihara, K. (1985). "Shear work and pore water pressure in undrained shear," *Soils and Foundations*, 25(3), 73-84.

Yamaguchi, Y., Kazama, M. and Kusakabe, S. (2002) "Online test of the seismic response at Kobe artificial island," *JSCE Journal of Geotechnical Engineering, No.701/III-58*, pp.181–195 (in Japanese).

Yamawaki, D., Hyodo, M., Nakata, Y., Murata, H., Yoshimoto, N. and Matsuoka, N. (2002). "Effect of particle shape on shear behaviour of sand," *Proceedings of the 37th Japan National Conference on Geotechnical Engineering*, 443-444 (in Japanese).

Yoshimoto, N., Hyodo, M., Nakata, Y., Murata, H., Hongo, T. and Ohnaka, A. (2005). "Particle characteristics of granulated coal ash as geomaterial," J*ournal of the Society of Materials Science*, 54(11), 1111-1116 (in Japanese).

Journal of Geotechnical and Geoenvironmental Engineering. Submitted September 5, 2012; accepted June 21, 2013; posted ahead of print June 24, 2013. doi:10.1061/(ASCE)GT.1943-5606.0000986

Yoshimoto, N., Hyodo, M., Nakata, Y., Murata, H., Hongo, T. and Ohnaka, A. (2006). "Liquefaction resistance of granulated coal ash," *Journal of Geotechnical Engineering,* JSCE, 62(1), 246-257 (in Japanese).

Yoshimoto, N., Hyodo, M., Nakata, Y. and Orense, R. P. (2007). "An examination of the utilization of granulated coal ash as geomaterial based on particle strength," *Tsuchi-to-Kiso*, 55(10), 23-25 (in Japanese).

Yoshimoto, N., Hyodo, M., Nakata, Y., Murata, H., Nishizono, T., Hongo, T., Ohnaka, A. and Saiai, K. (2008). "Cyclic shear characteristics of soil mixed with granulated coal ash," *Journal of the Society of Materials Science*, 57(1), 71-76 (in Japanese).

Journal of Geotechnical and Geoenvironmental Engineering. Submitted September 5, 2012; accepted June 21, 2013; posted ahead of print June 24, 2013. doi:10.1061/(ASCE)GT.1943-5606.0000986

LIST OF TABLES

LIST OF FIGURES

Journal of Geotechnical and Geoenvironmental Engineering. Submitted September 5, 2012; accepted June 21, 2013; posted ahead of print June 24, 2013. doi:10.1061/(ASCE)GT.1943-5606.0000986

Journal of Geotechnical and Geoenvironmental Engineering. Submitted September 5, 2012; accepted June 21, 2013; posted ahead of print June 24, 2013. doi:10.1061/(ASCE)GT.1943-5606.0000986

Table 1

Sample	ρ_s (g/cm^3)	e_{max}	e_{min}	d_{50} (mm)	R_c	A_r
Granulated Coal Ash	2.28	2.280	1.512	0.368	1.287	1.249
P.I. Masado	2.62	0.967	0.491	0.509	1.251	1.445
Aio	2.63	0.958	0.582	1.138	1.274	1.557
Wakasa	2.65	1.105	0.680	0.311	1.272	1.506
Toyoura	2.64	0.973	0.635	0.200	1.203	1.454
Iwakuni clay	2.61	-	-	0.007	-	-
Shirasu (F_c=10%)	2.38	1.459	0.799	0.323	1.402	1.657

Figure 1

Journal of Geotechnical and Geoenvironmental Engineering. Submitted September 5, 2012; accepted June 21, 2013;
posted ahead of print June 24, 2013. doi:10.1061/(ASCE)GT.1943-5606.0000986

Figure 2

Journal of Geotechnical and Geoenvironmental Engineering. Submitted September 5, 2012; accepted June 21, 2013;
posted ahead of print June 24, 2013. doi:10.1061/(ASCE)GT.1943-5606.0000986

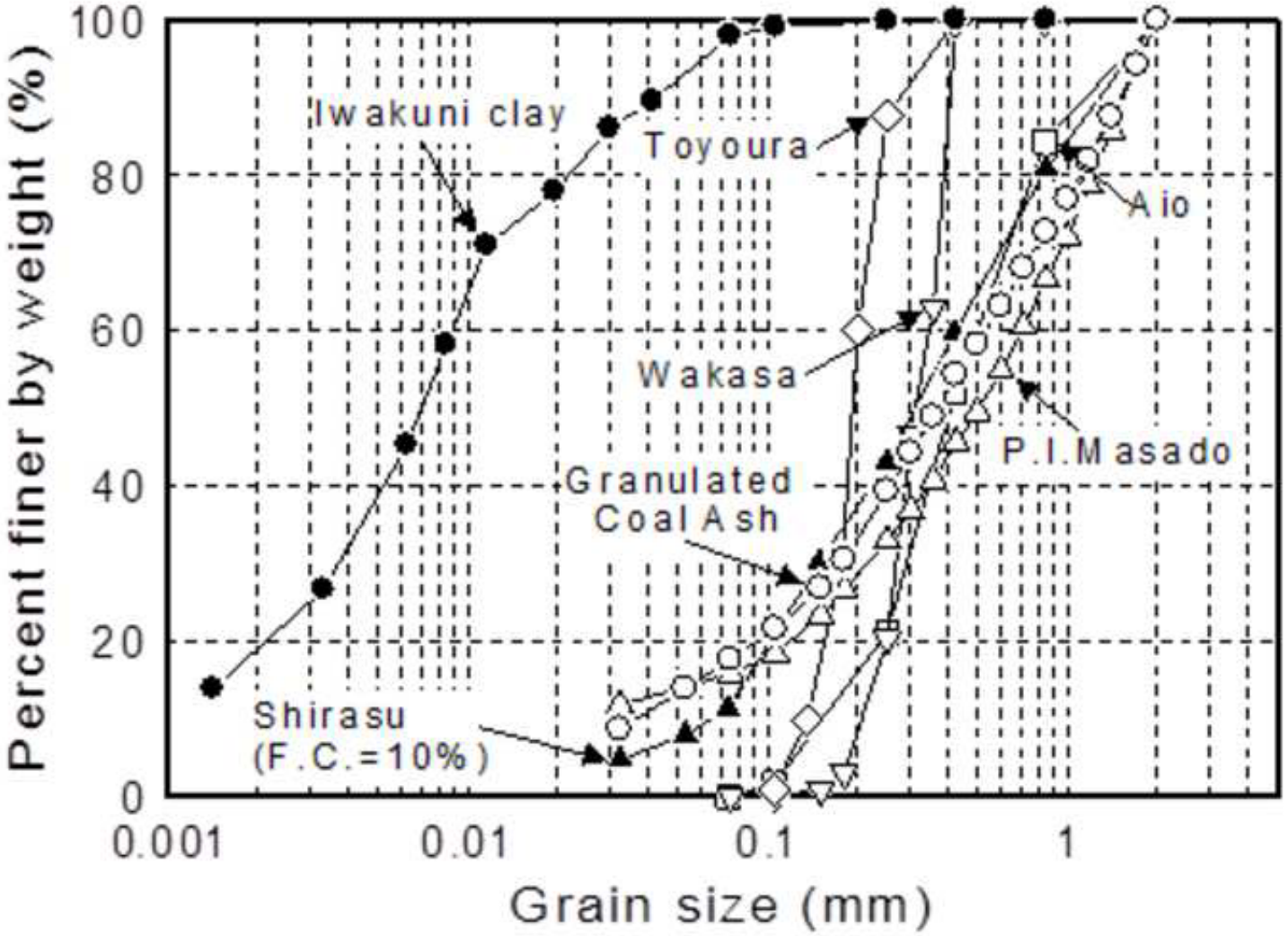

Figure 3

Journal of Geotechnical and Geoenvironmental Engineering. Submitted September 5, 2012; accepted June 21, 2013;
posted ahead of print June 24, 2013. doi:10.1061/(ASCE)GT.1943-5606.0000986

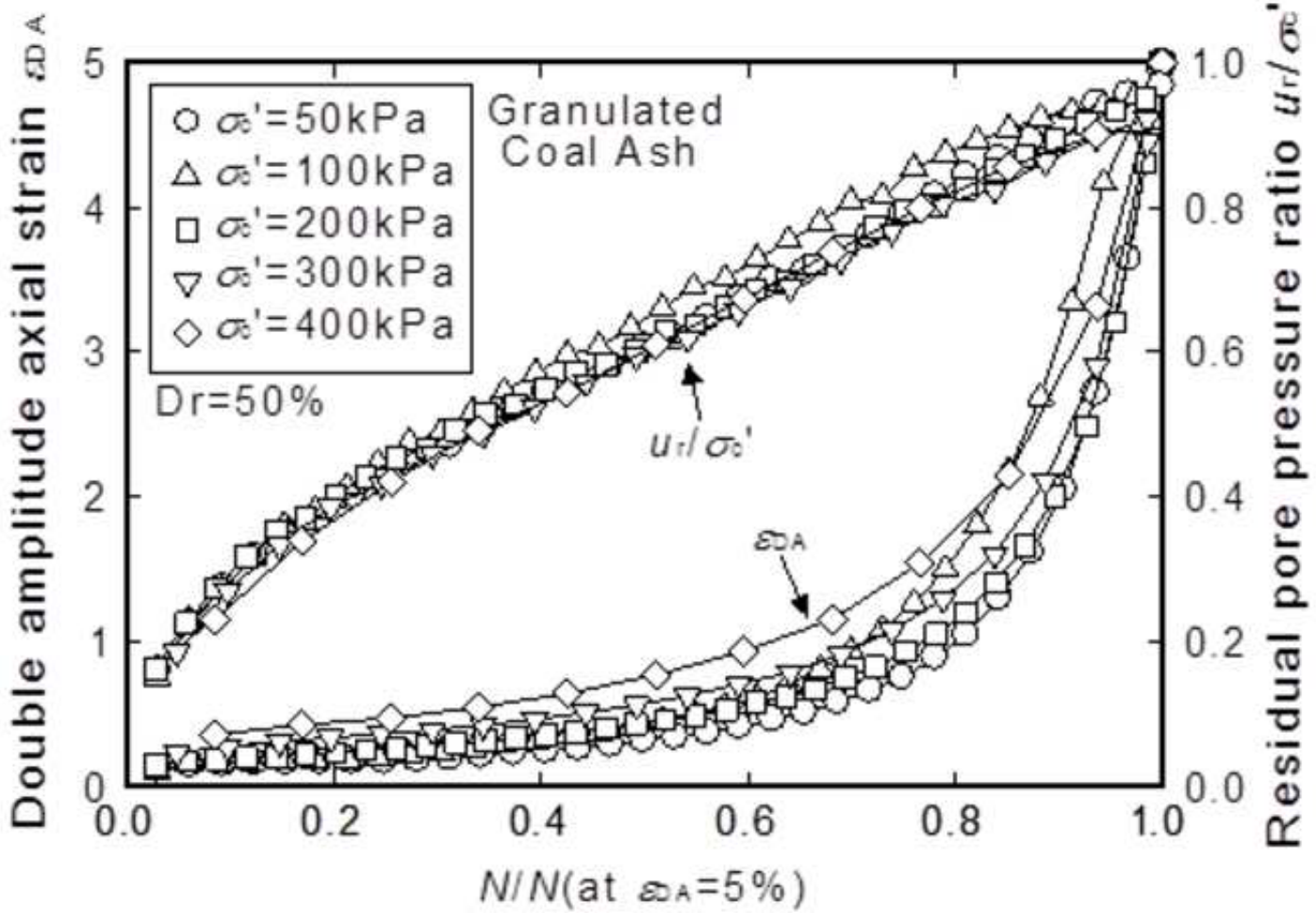

Figure 4

Journal of Geotechnical and Geoenvironmental Engineering. Submitted September 5, 2012; accepted June 21, 2013;
posted ahead of print June 24, 2013. doi:10.1061/(ASCE)GT.1943-5606.0000986

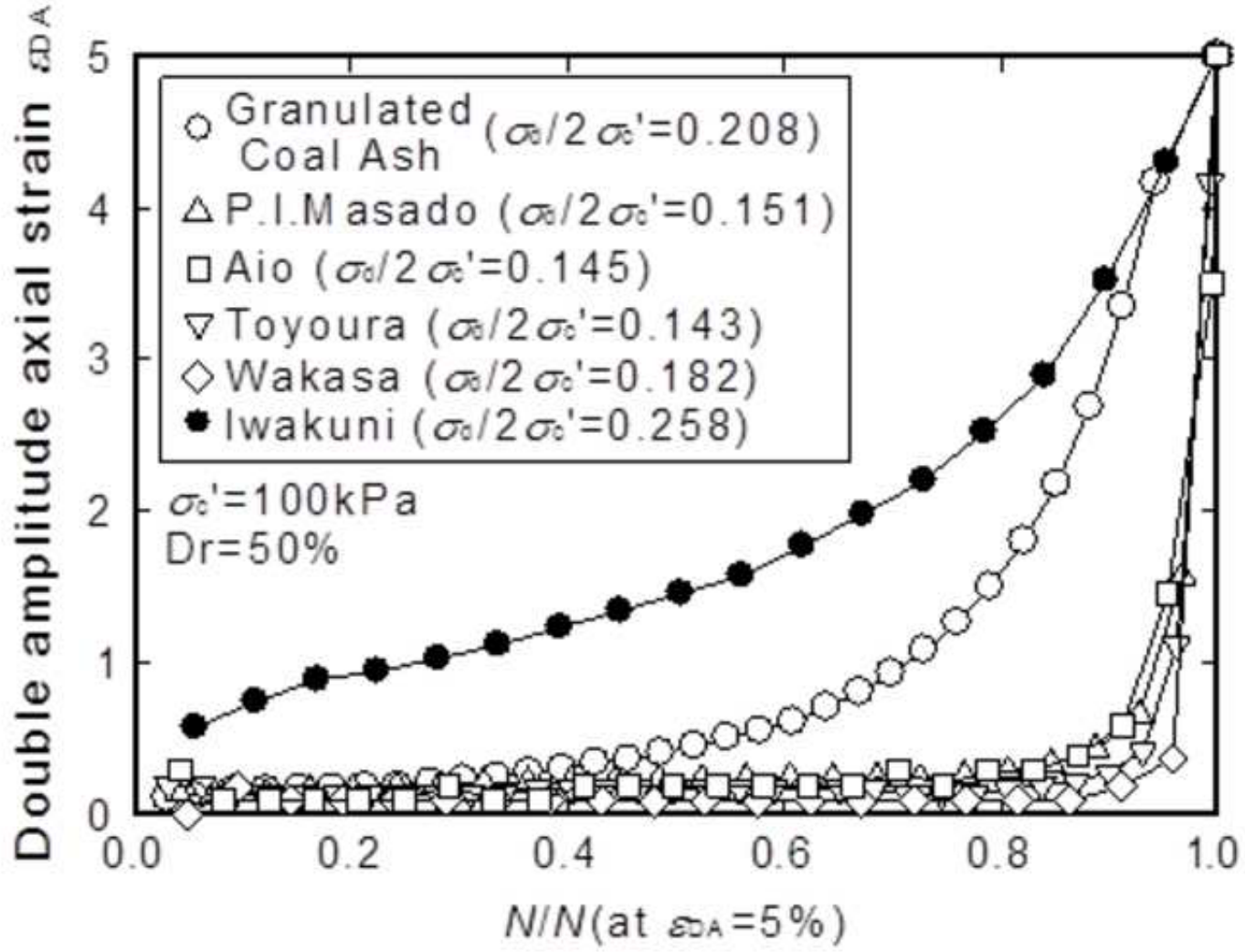

Figure 5

Journal of Geotechnical and Geoenvironmental Engineering. Submitted September 5, 2012; accepted June 21, 2013;
posted ahead of print June 24, 2013. doi:10.1061/(ASCE)GT.1943-5606.0000986

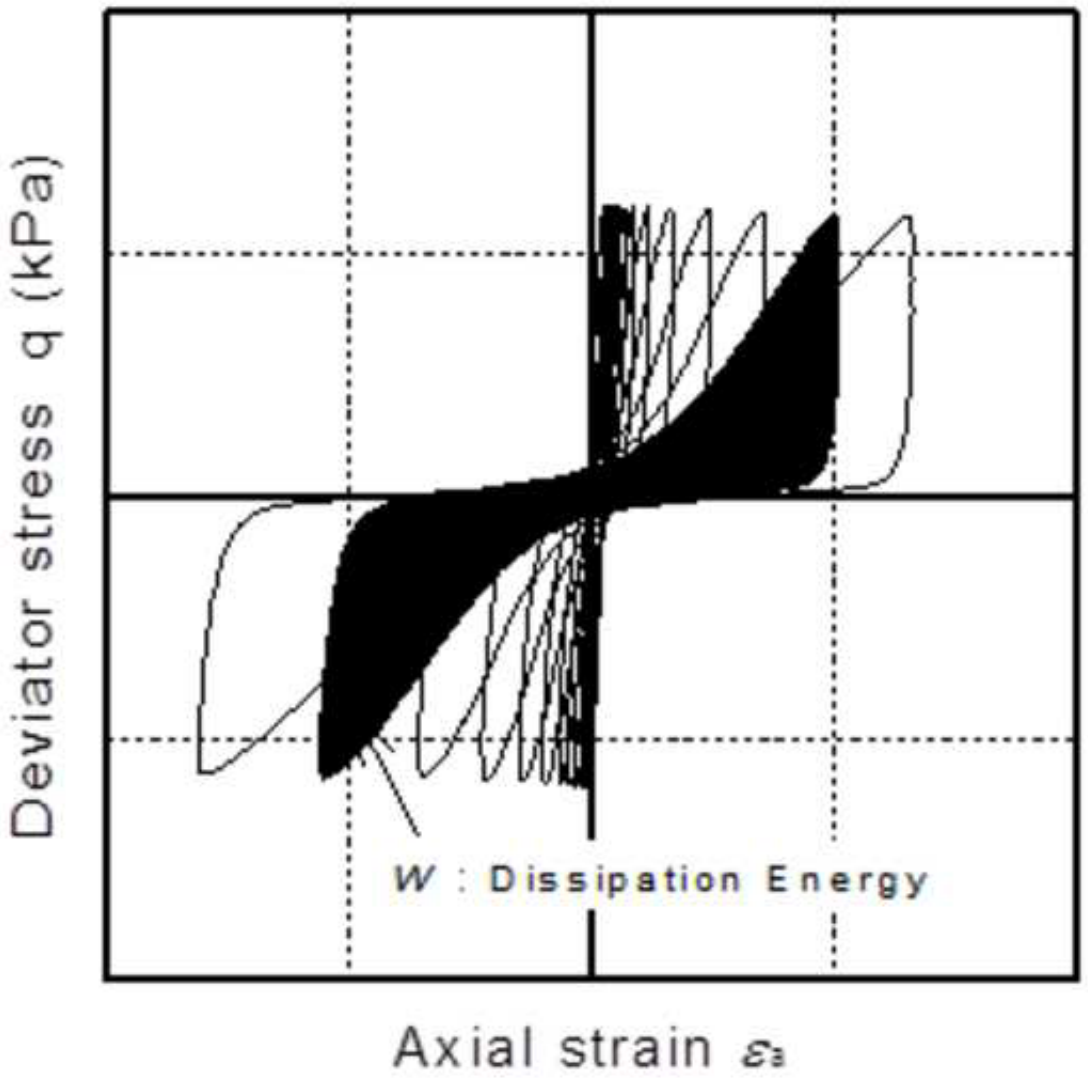

Figure 6

Journal of Geotechnical and Geoenvironmental Engineering. Submitted September 5, 2012; accepted June 21, 2013;
posted ahead of print June 24, 2013. doi:10.1061/(ASCE)GT.1943-5606.0000986

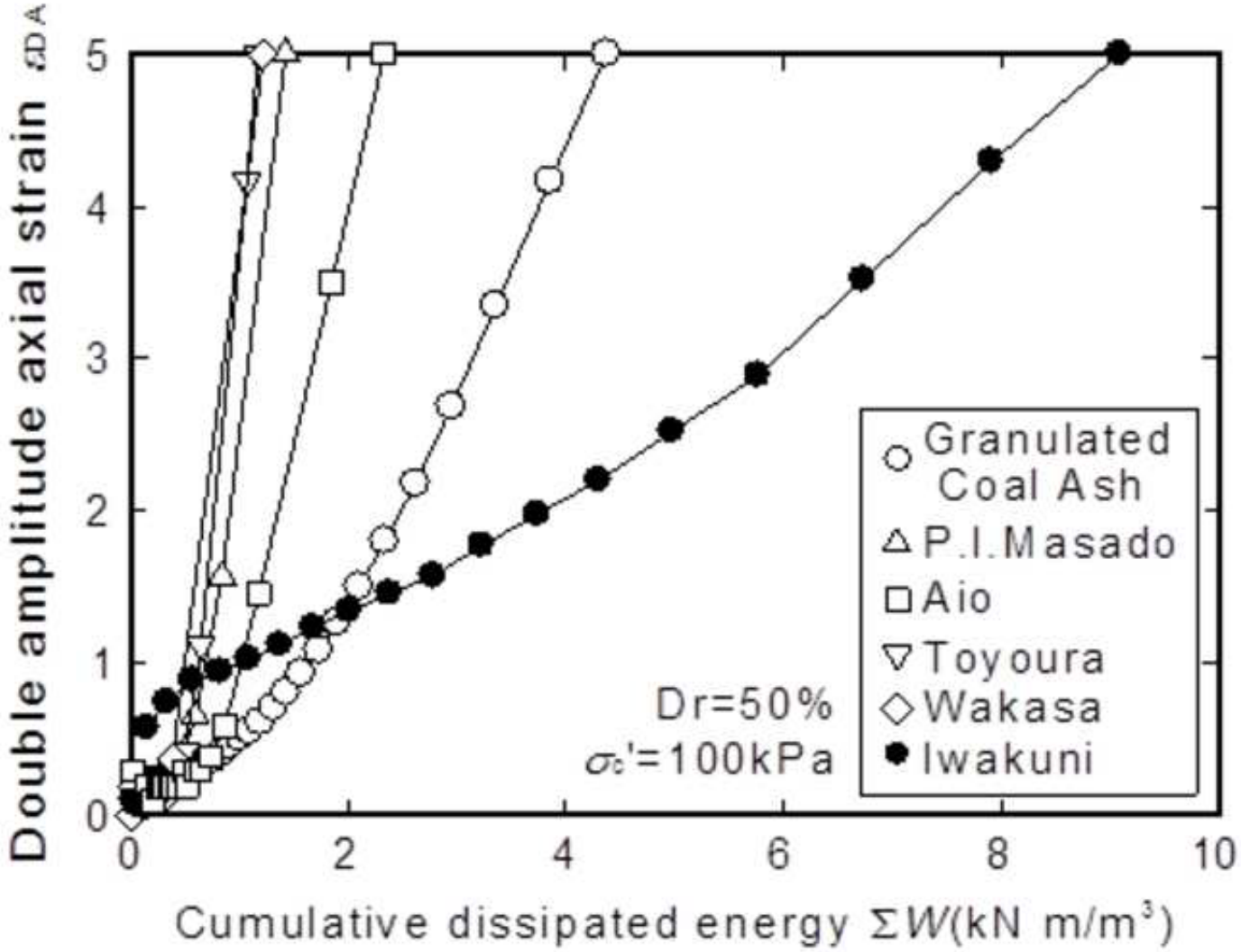

Figure 7

Journal of Geotechnical and Geoenvironmental Engineering. Submitted September 5, 2012; accepted June 21, 2013;
posted ahead of print June 24, 2013. doi:10.1061/(ASCE)GT.1943-5606.0000986

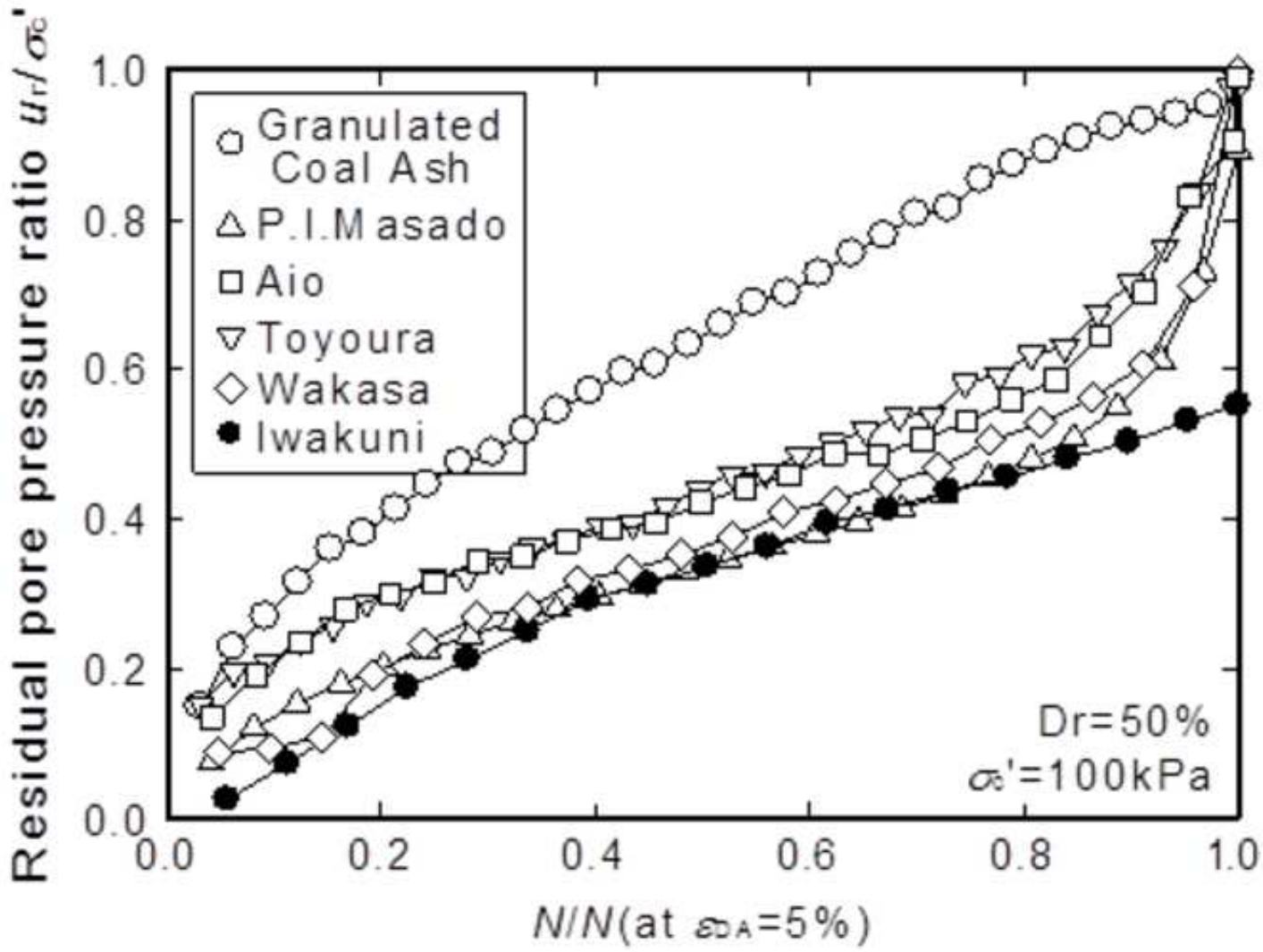

Figure 8

Journal of Geotechnical and Geoenvironmental Engineering. Submitted September 5, 2012; accepted June 21, 2013;
posted ahead of print June 24, 2013. doi:10.1061/(ASCE)GT.1943-5606.0000986

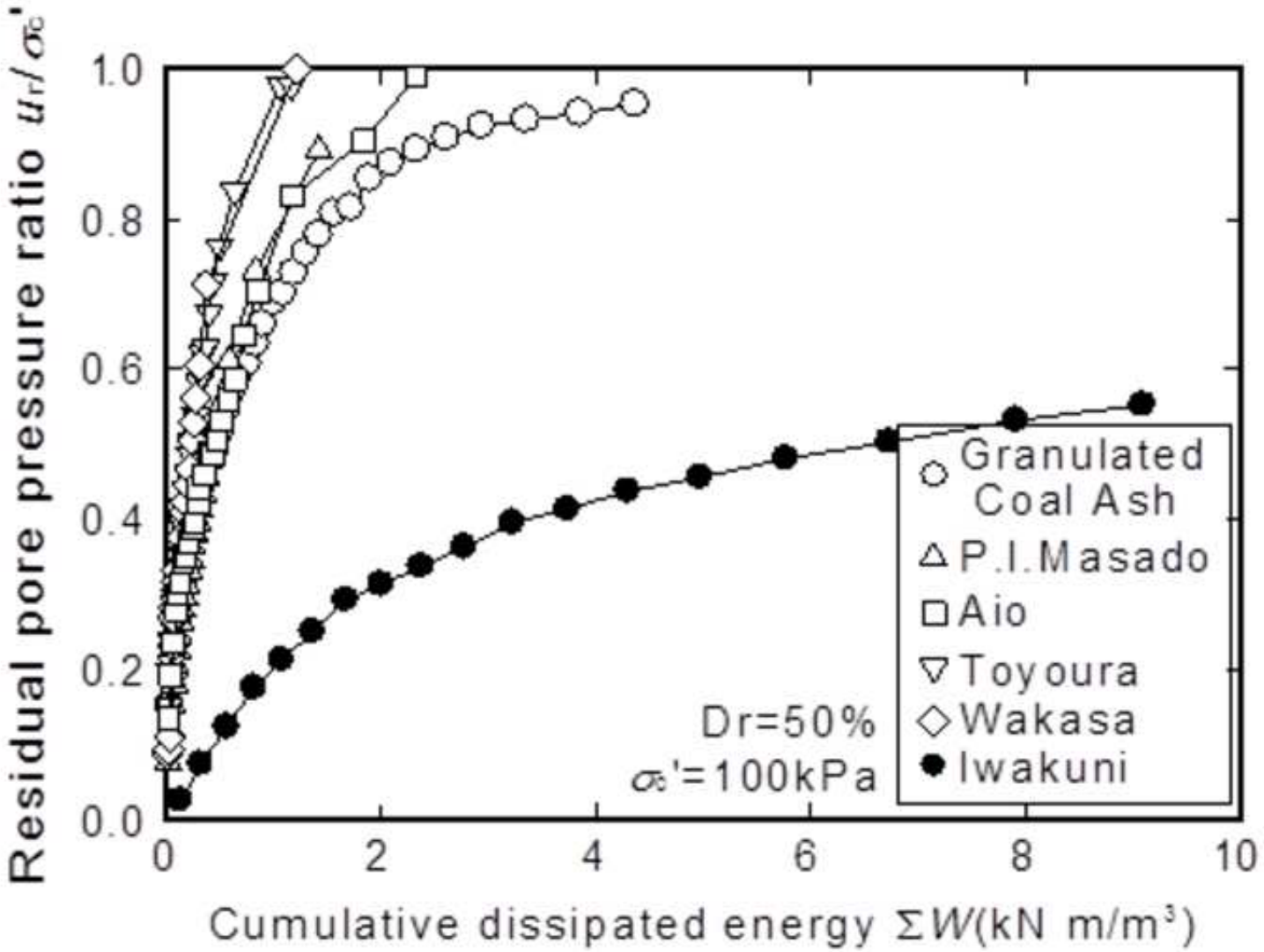

Figure 9a

Journal of Geotechnical and Geoenvironmental Engineering. Submitted September 5, 2012; accepted June 21, 2013;
posted ahead of print June 24, 2013. doi:10.1061/(ASCE)GT.1943-5606.0000986

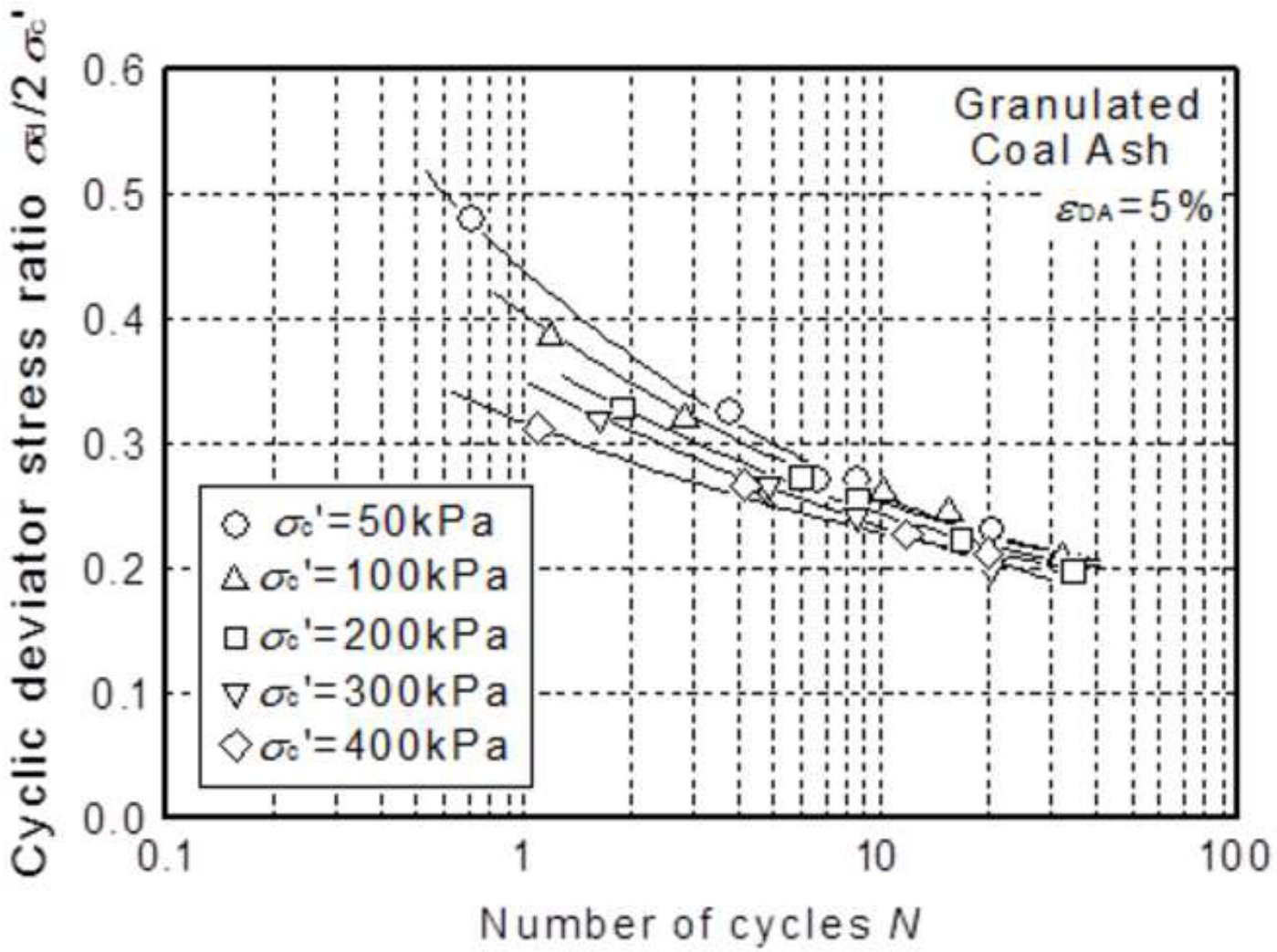

Figure 9b

Journal of Geotechnical and Geoenvironmental Engineering. Submitted September 5, 2012; accepted June 21, 2013;
posted ahead of print June 24, 2013. doi:10.1061/(ASCE)GT.1943-5606.0000986

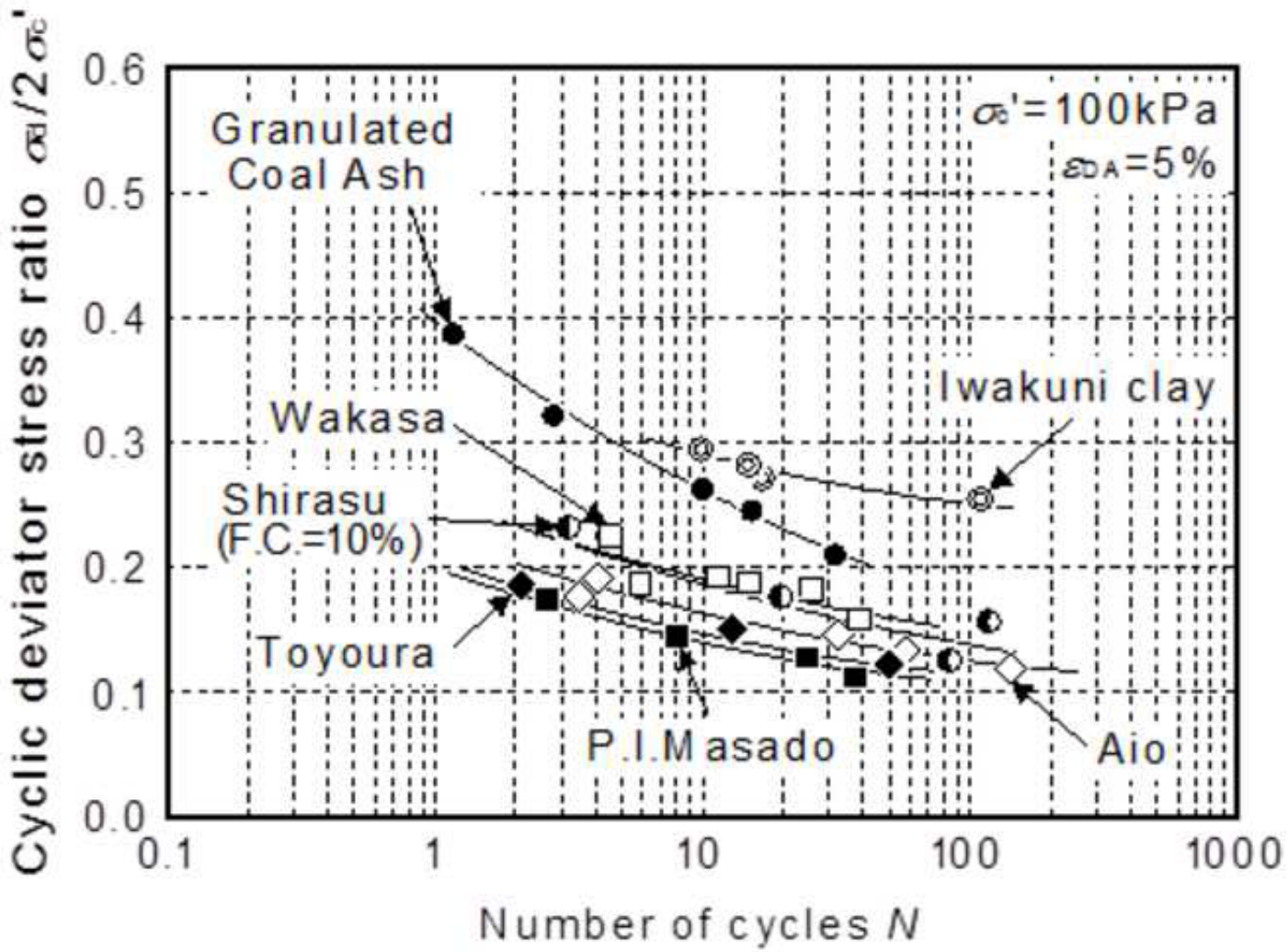

Figure 10

Journal of Geotechnical and Geoenvironmental Engineering. Submitted September 5, 2012; accepted June 21, 2013;
posted ahead of print June 24, 2013. doi:10.1061/(ASCE)GT.1943-5606.0000986

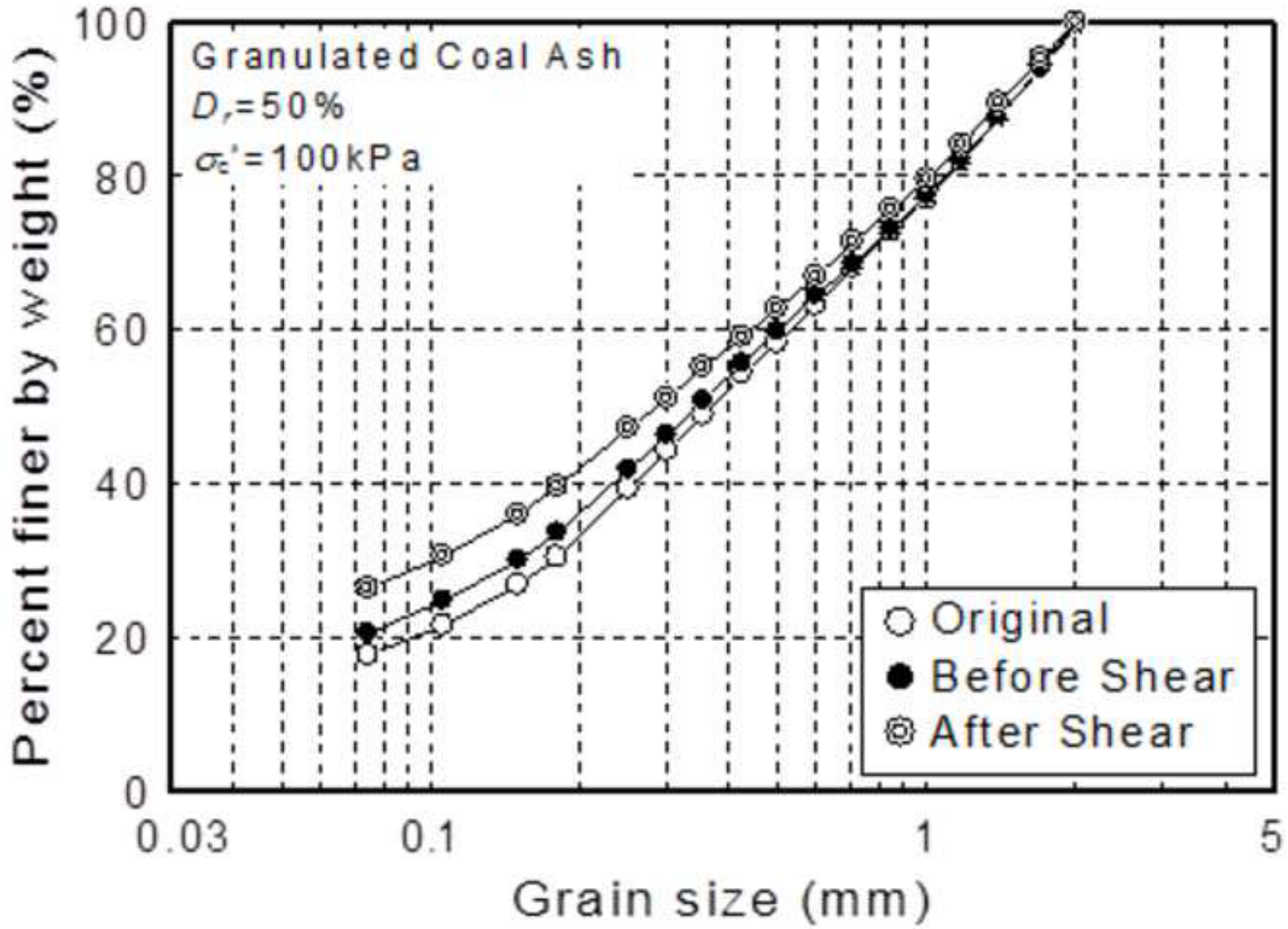

Figure 11a

Journal of Geotechnical and Geoenvironmental Engineering. Submitted September 5, 2012; accepted June 21, 2013;
posted ahead of print June 24, 2013. doi:10.1061/(ASCE)GT.1943-5606.0000986

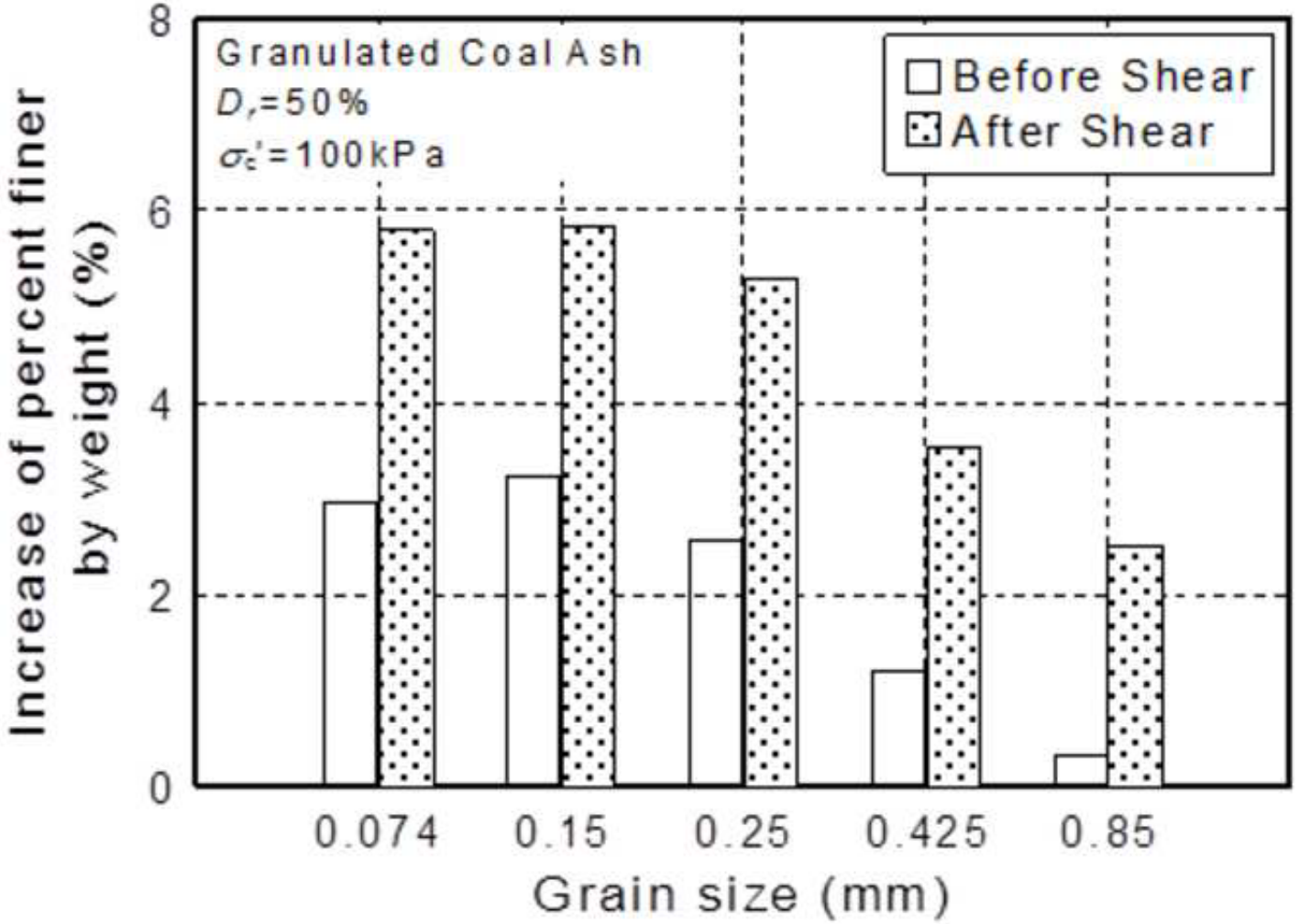

Figure 11b

Journal of Geotechnical and Geoenvironmental Engineering. Submitted September 5, 2012; accepted June 21, 2013;
posted ahead of print June 24, 2013. doi:10.1061/(ASCE)GT.1943-5606.0000986

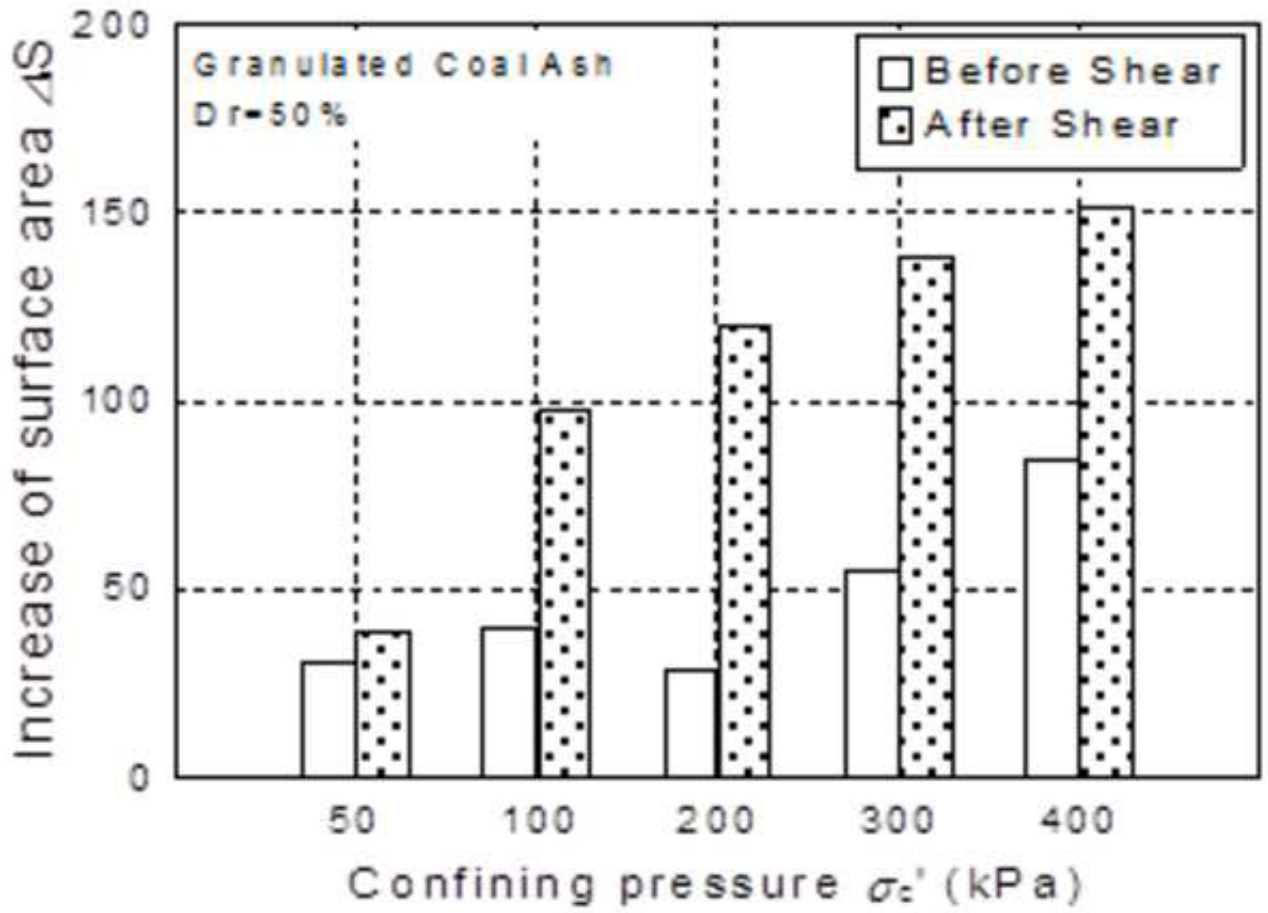

Figure 12

Journal of Geotechnical and Geoenvironmental Engineering. Submitted September 5, 2012; accepted June 21, 2013;
posted ahead of print June 24, 2013. doi:10.1061/(ASCE)GT.1943-5606.0000986

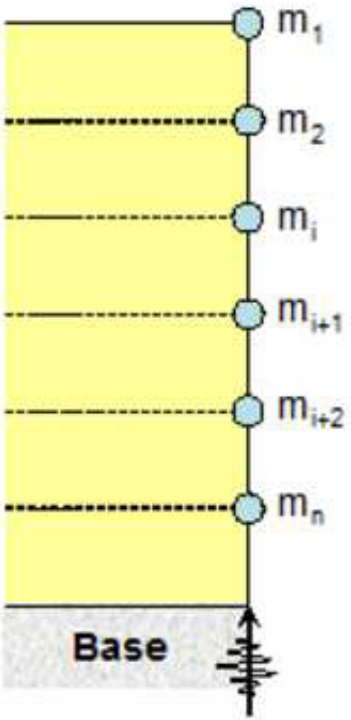

(a)

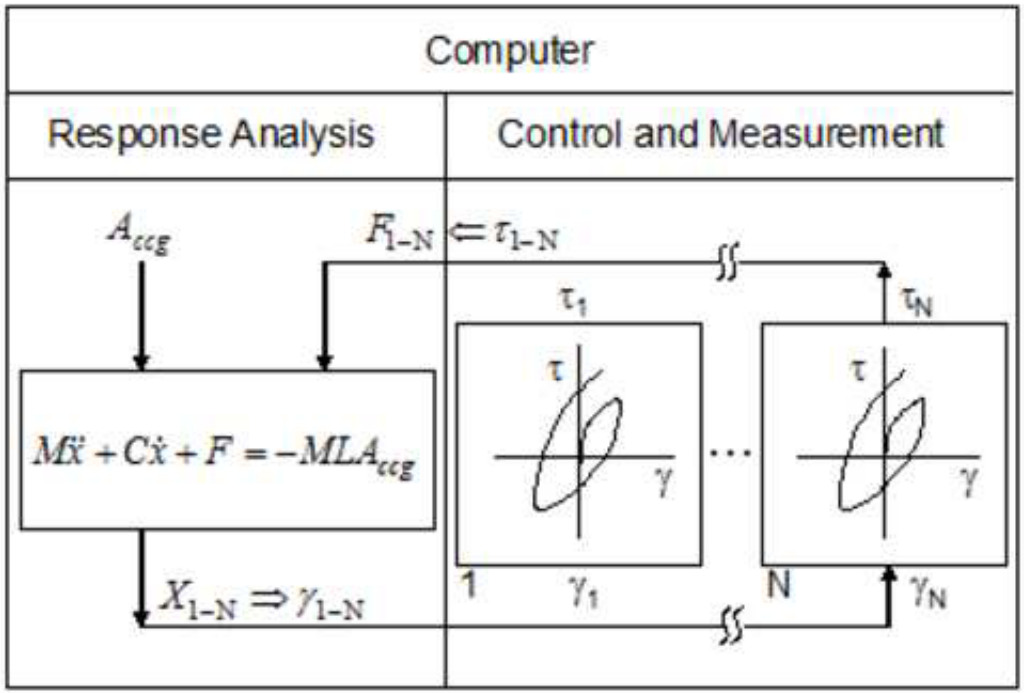

(b)

Figure 13

Journal of Geotechnical and Geoenvironmental Engineering. Submitted September 5, 2012; accepted June 21, 2013;
posted ahead of print June 24, 2013. doi:10.1061/(ASCE)GT.1943-5606.0000986

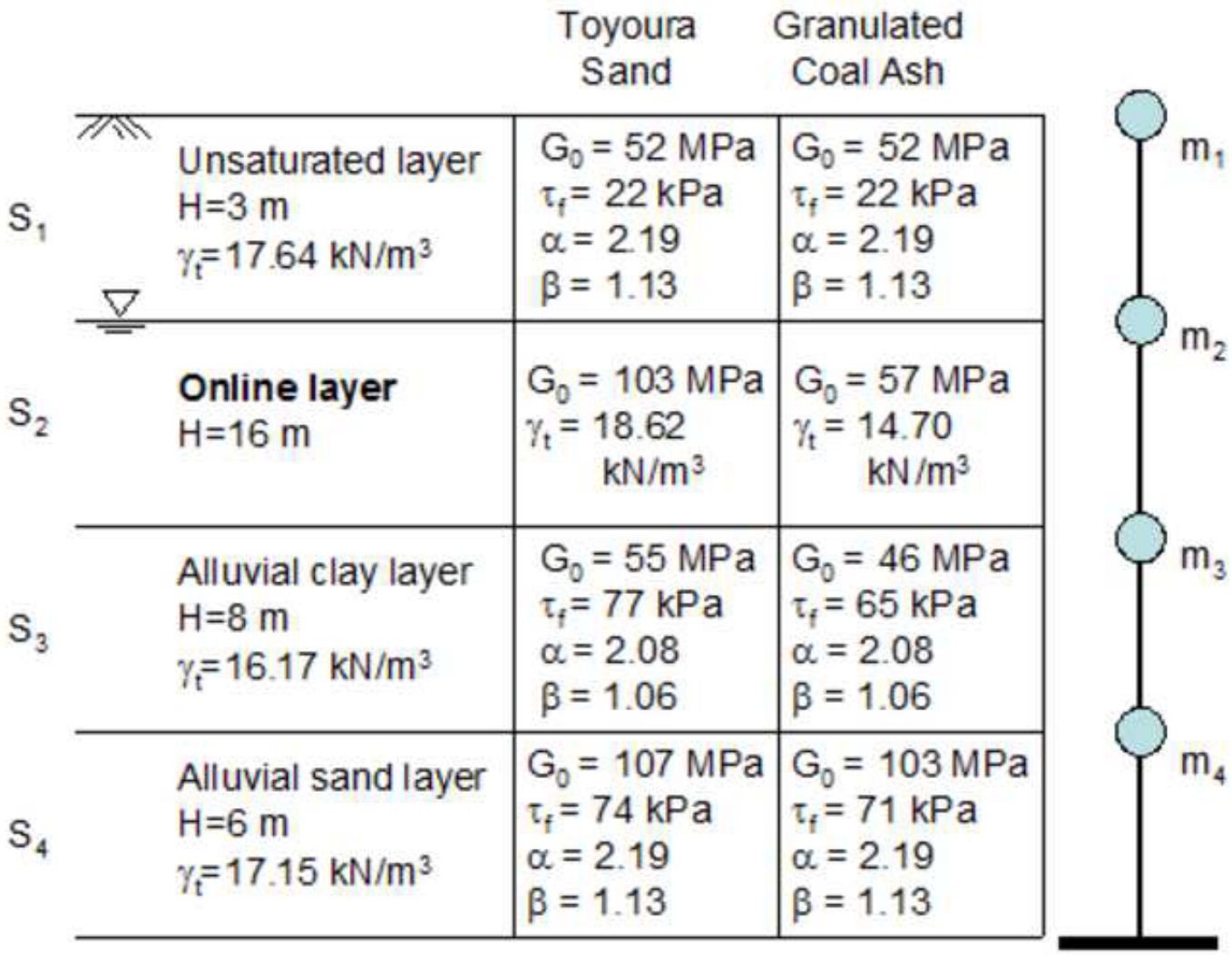

Figure 14

Journal of Geotechnical and Geoenvironmental Engineering. Submitted September 5, 2012; accepted June 21, 2013;
posted ahead of print June 24, 2013. doi:10.1061/(ASCE)GT.1943-5606.0000986

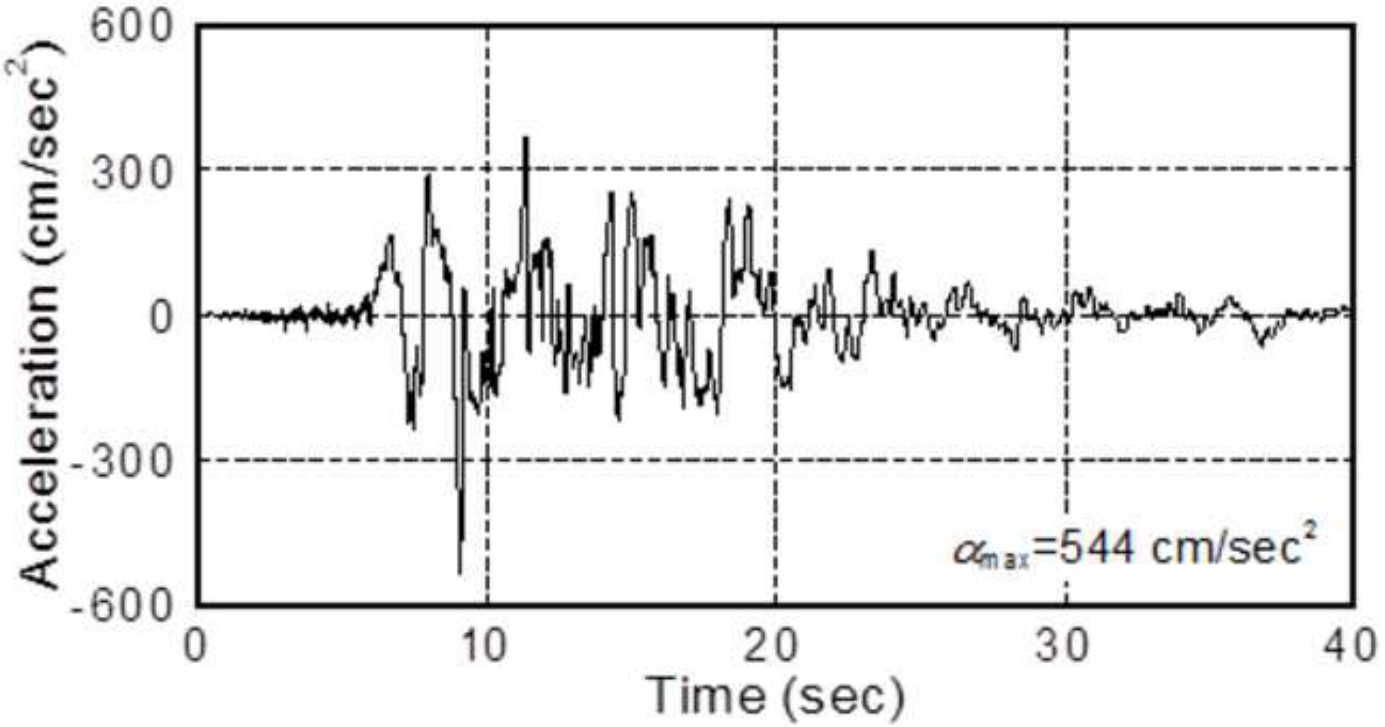

Figure 15a

Journal of Geotechnical and Geoenvironmental Engineering. Submitted September 5, 2012; accepted June 21, 2013; posted ahead of print June 24, 2013. doi:10.1061/(ASCE)GT.1943-5606.0000986

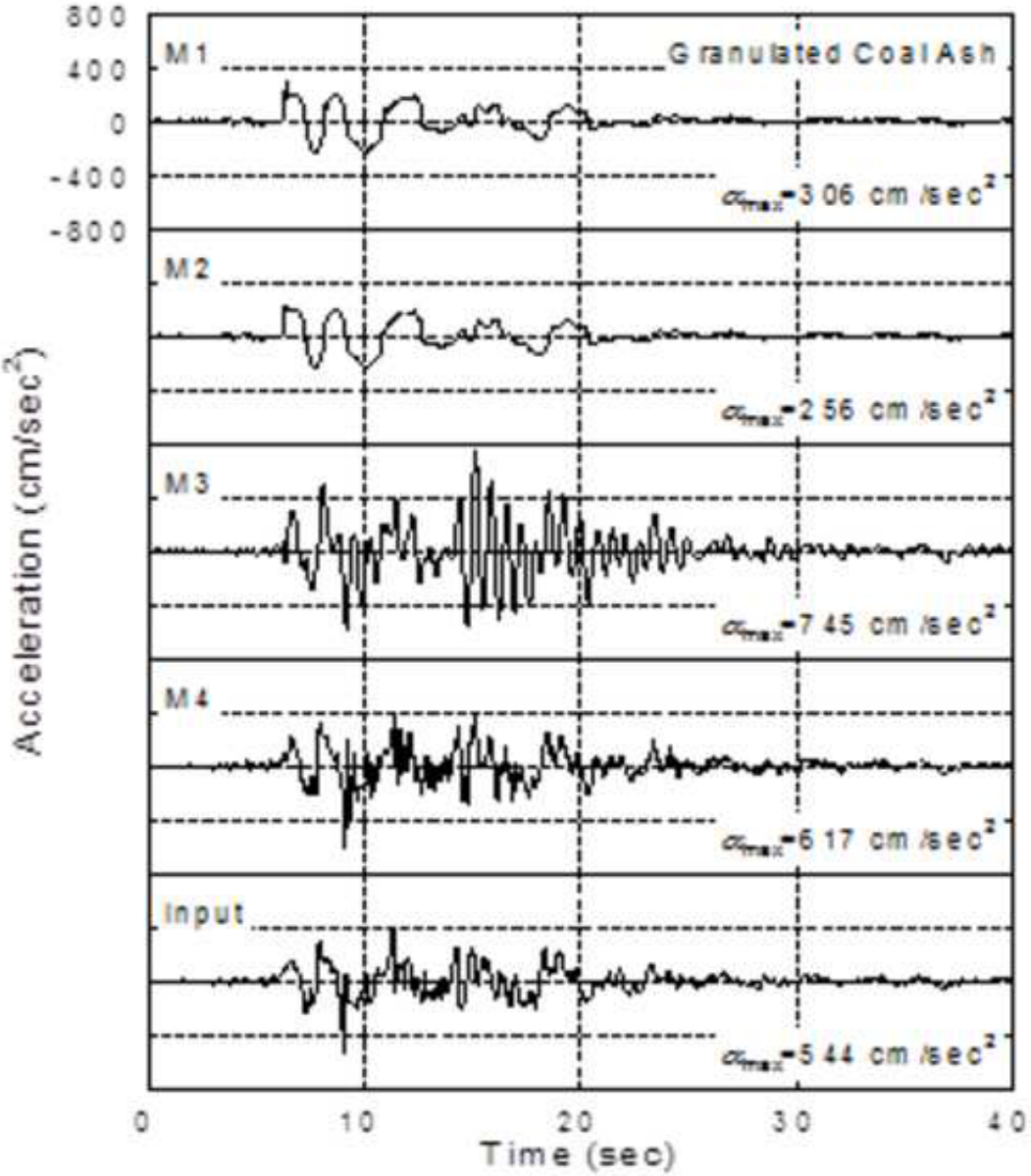

Figure 15b

Journal of Geotechnical and Geoenvironmental Engineering. Submitted September 5, 2012; accepted June 21, 2013; posted ahead of print June 24, 2013. doi:10.1061/(ASCE)GT.1943-5606.0000986

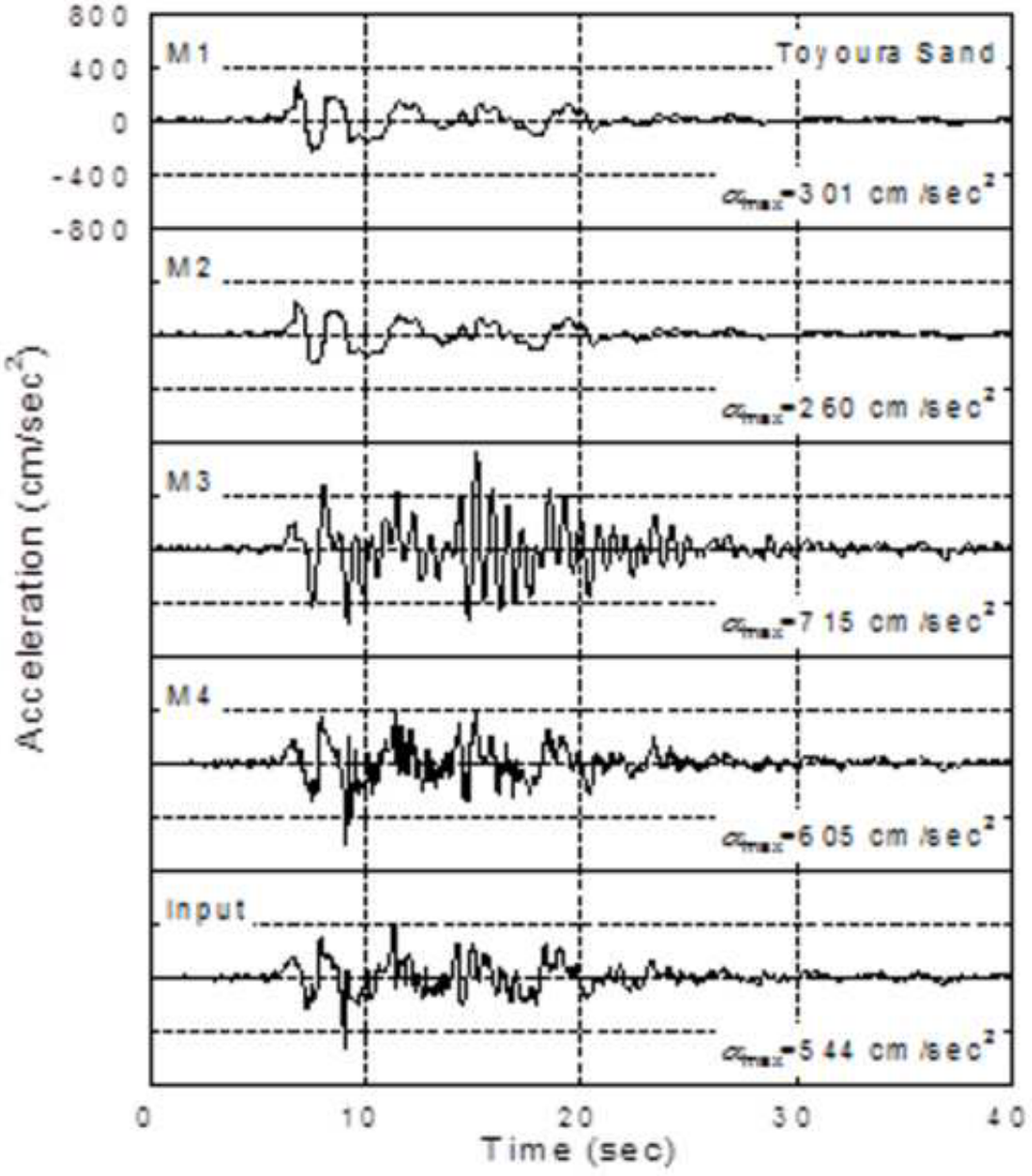

Figure 16a

Journal of Geotechnical and Geoenvironmental Engineering. Submitted September 5, 2012; accepted June 21, 2013;
posted ahead of print June 24, 2013. doi:10.1061/(ASCE)GT.1943-5606.0000986

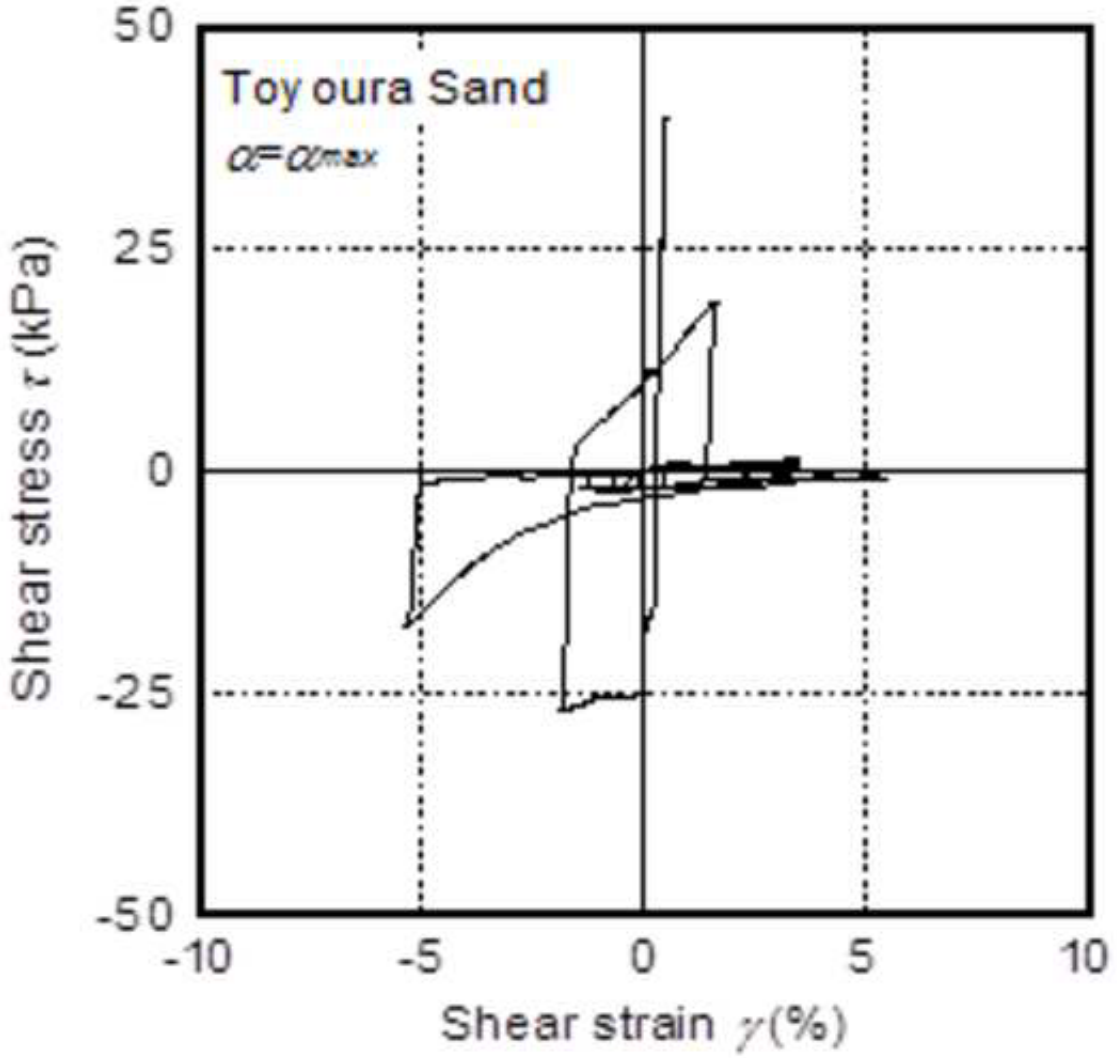

Figure 16b

Journal of Geotechnical and Geoenvironmental Engineering. Submitted September 5, 2012; accepted June 21, 2013;
posted ahead of print June 24, 2013. doi:10.1061/(ASCE)GT.1943-5606.0000986

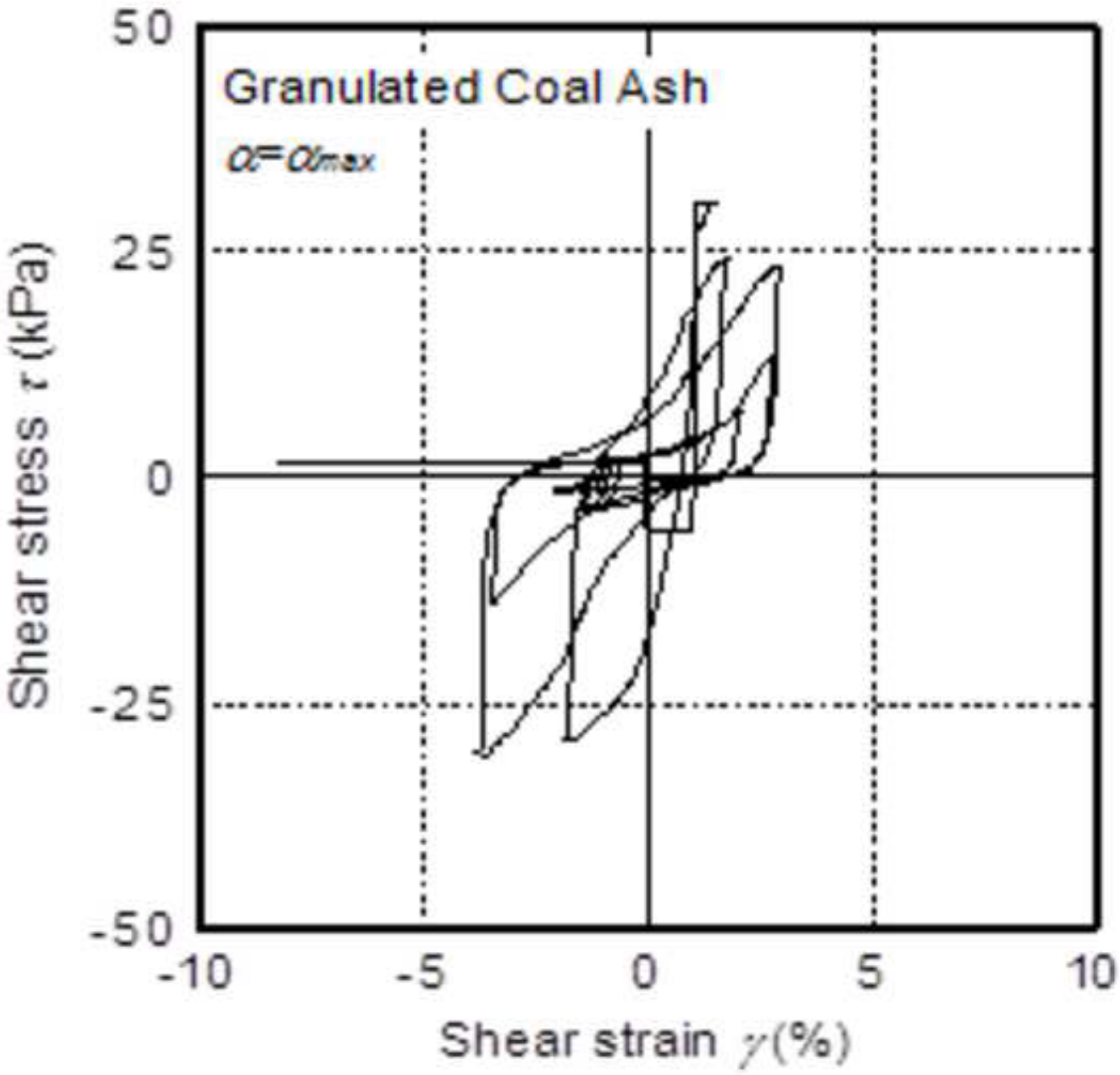

Figure 17a

Journal of Geotechnical and Geoenvironmental Engineering. Submitted September 5, 2012; accepted June 21, 2013;
posted ahead of print June 24, 2013. doi:10.1061/(ASCE)GT.1943-5606.0000986

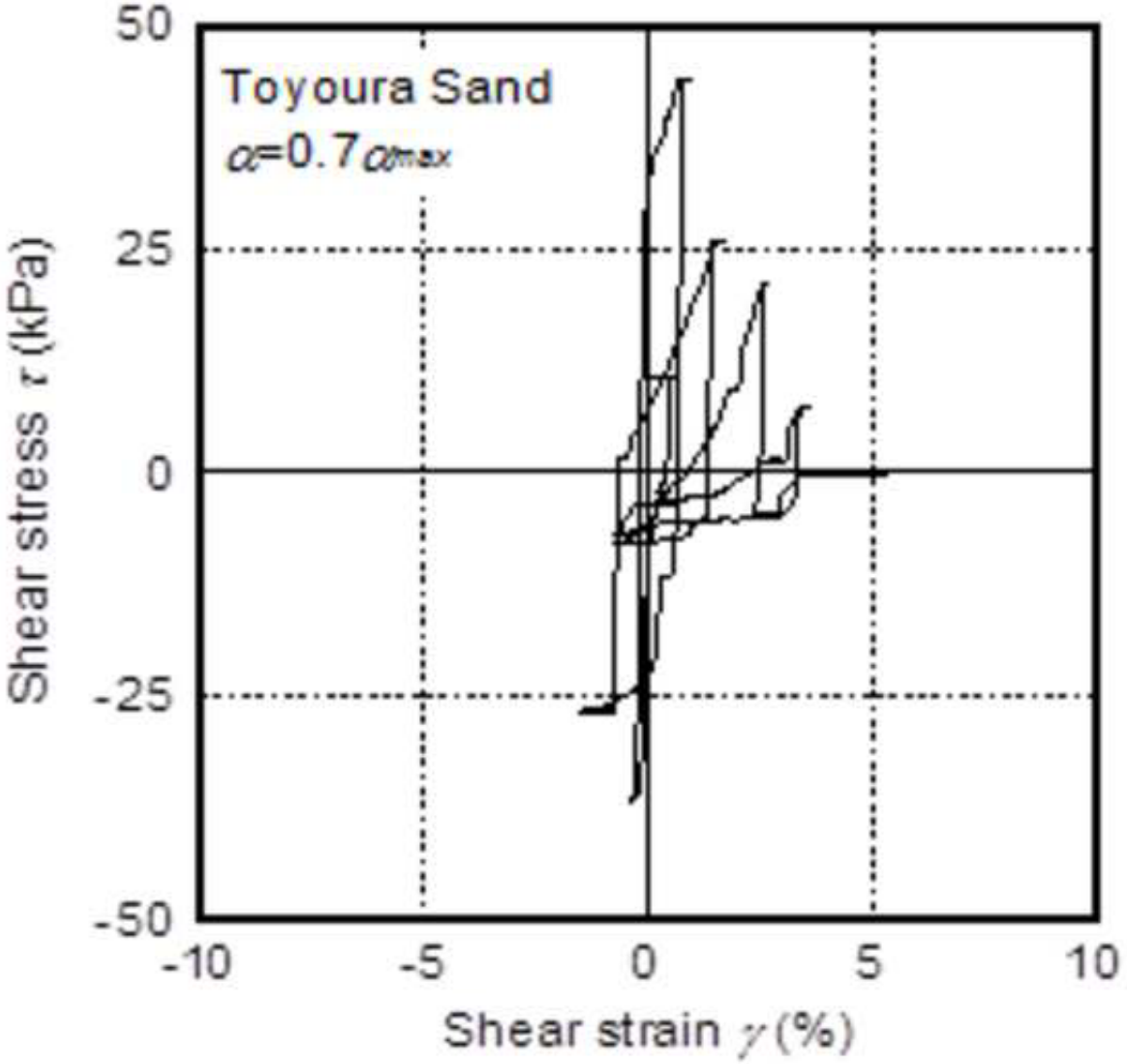

Figure 17b

Journal of Geotechnical and Geoenvironmental Engineering. Submitted September 5, 2012; accepted June 21, 2013;
posted ahead of print June 24, 2013. doi:10.1061/(ASCE)GT.1943-5606.0000986

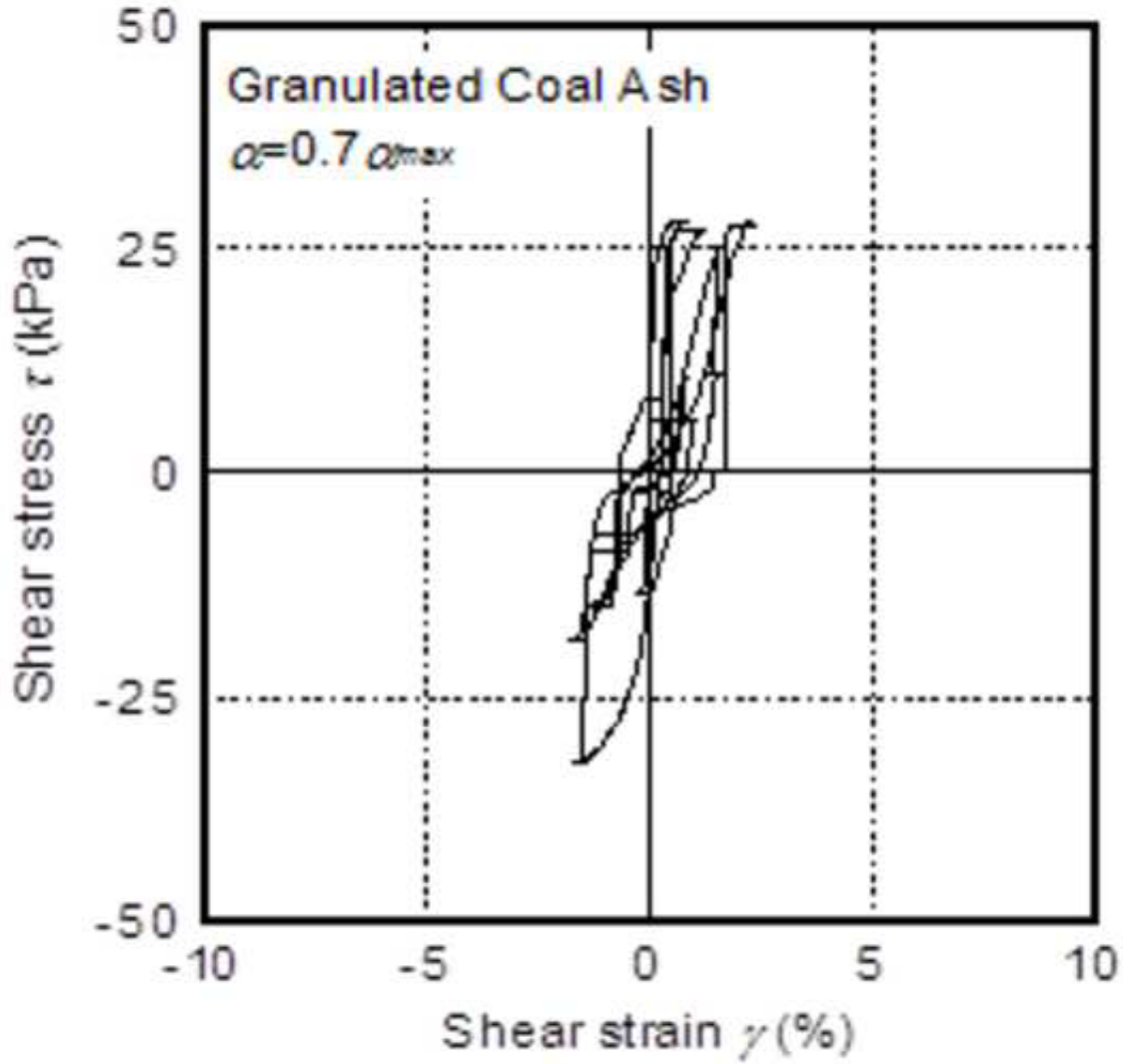

Figure 18a

Journal of Geotechnical and Geoenvironmental Engineering. Submitted September 5, 2012; accepted June 21, 2013;
posted ahead of print June 24, 2013. doi:10.1061/(ASCE)GT.1943-5606.0000986

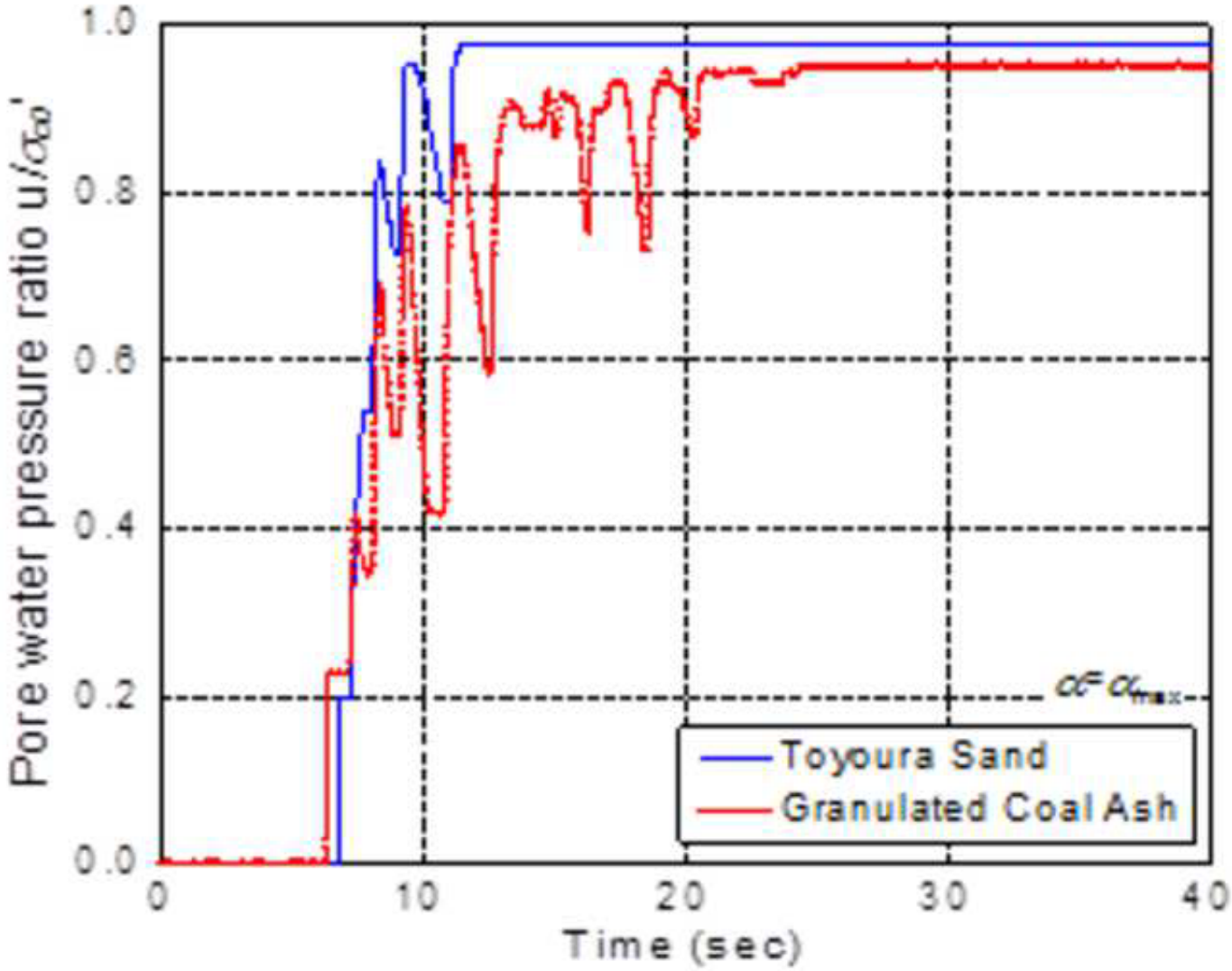

Figure 18b

Journal of Geotechnical and Geoenvironmental Engineering. Submitted September 5, 2012; accepted June 21, 2013;
posted ahead of print June 24, 2013. doi:10.1061/(ASCE)GT.1943-5606.0000986

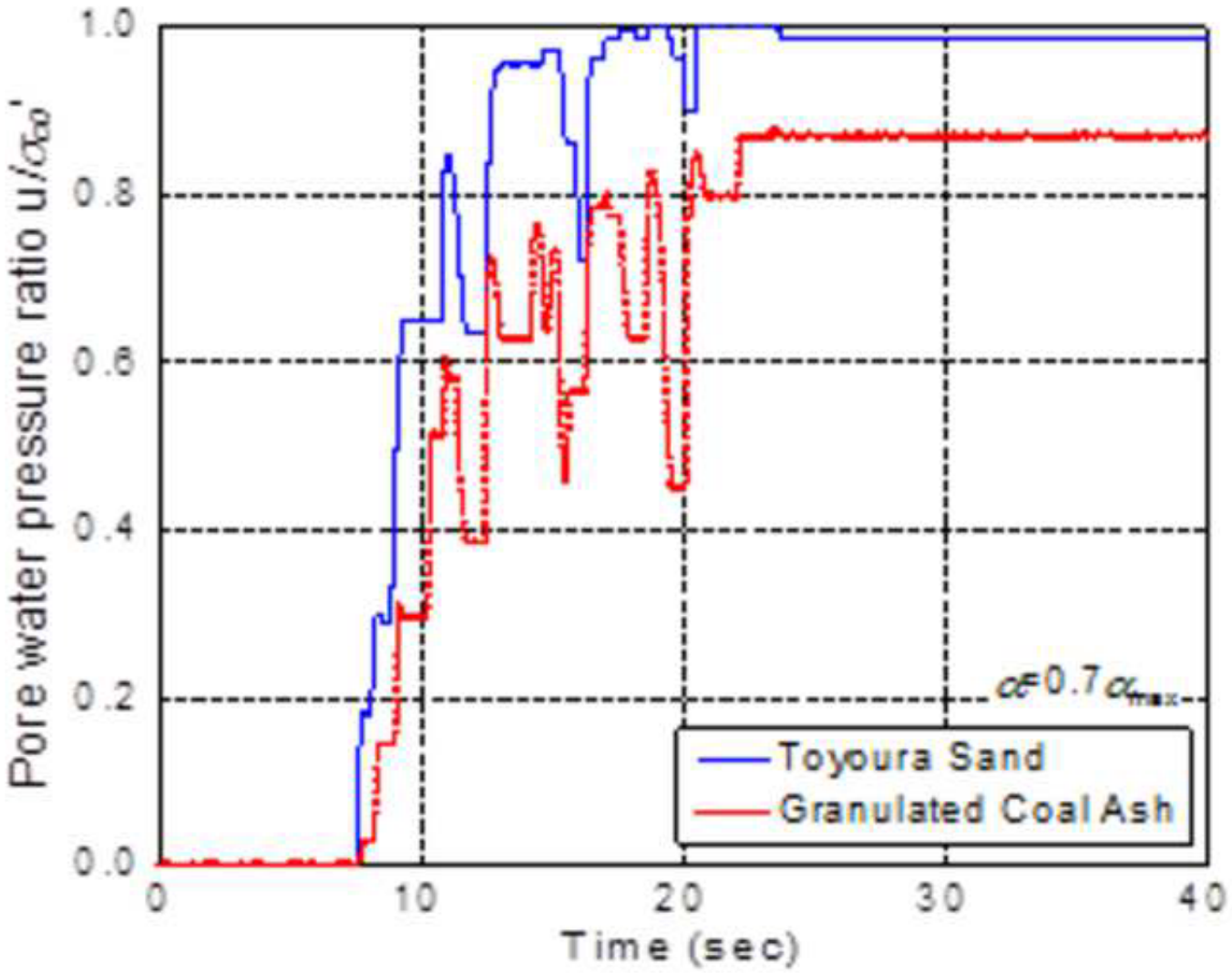

Figure 19a

Journal of Geotechnical and Geoenvironmental Engineering. Submitted September 5, 2012; accepted June 21, 2013;
posted ahead of print June 24, 2013. doi:10.1061/(ASCE)GT.1943-5606.0000986

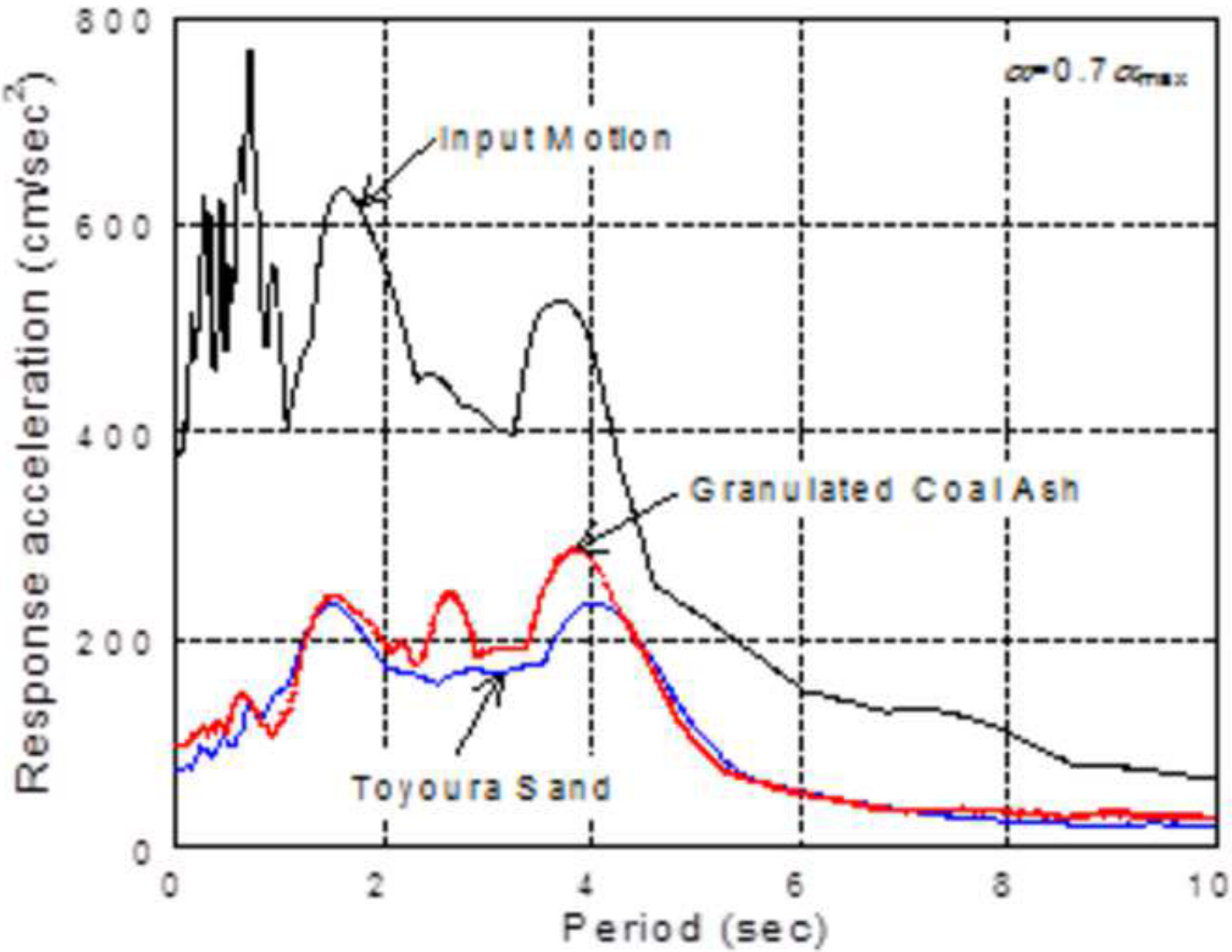

Figure 19b

Journal of Geotechnical and Geoenvironmental Engineering. Submitted September 5, 2012; accepted June 21, 2013;
posted ahead of print June 24, 2013. doi:10.1061/(ASCE)GT.1943-5606.0000986

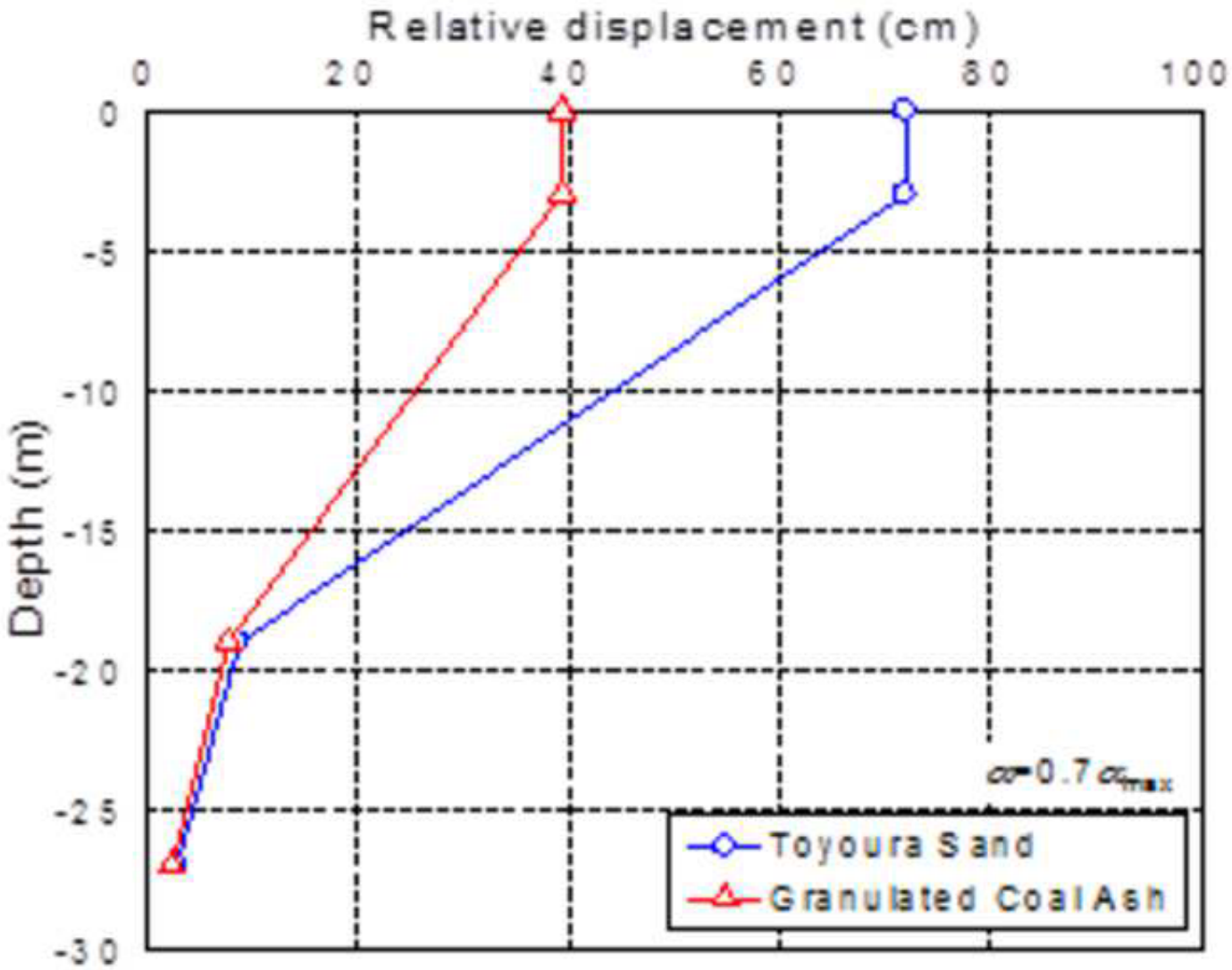

Figure 20

Journal of Geotechnical and Geoenvironmental Engineering. Submitted September 5, 2012; accepted June 21, 2013;
posted ahead of print June 24, 2013. doi:10.1061/(ASCE)GT.1943-5606.0000986